International Geology Review
Publication details, including instructions for authors and subscription information:
http://www.tandfonline.com/loi/tigr20

Geochemical and Sr-Nd-Pb isotopic compositions of Mesozoic mafic dikes from the Gan-Hang tectonic belt, South China: petrogenesis and geodynamic significance

Youqiang Qi [a], Ruizhong Hu [a], Shen Liu [a], Ian M. Coulson [b], Huawen Qi [a], Jianji Tian [c], Caixia Feng [a] & Tao Wang [d]

[a] State Key Laboratory of Ore Deposit Geochemistry, Institute of Geochemistry, Chinese Academy of Sciences, Guiyang, 550002, PR China

[b] Solid Earth Studies Laboratory, Department of Geology, University of Regina, Regina, Saskatchewan, Canada, S4S 0A2

[c] Beijing Research Institute of Uranium Geology, Beijng, 100029, PR China

[d] College of Earth Science, Chengdu University of Technology, Chengdu, 610059, PR China

Published online: 28 Oct 2011.

International Geology Review
Vol. 54, No. 8, June 2012, 920–939

Taylor & Francis
Taylor & Francis Group

Geochemical and Sr–Nd–Pb isotopic compositions of Mesozoic mafic dikes from the Gan-Hang tectonic belt, South China: petrogenesis and geodynamic significance

Youqiang Qi[a], Ruizhong Hu[a]*, Shen Liu[a], Ian M. Coulson[b], Huawen Qi[a], Jianji Tian[c], Caixia Feng[a] and Tao Wang[d]

[a]*State Key Laboratory of Ore Deposit Geochemistry, Institute of Geochemistry, Chinese Academy of Sciences, Guiyang 550002, PR China;* [b]*Solid Earth Studies Laboratory, Department of Geology, University of Regina, Regina, Saskatchewan, Canada, S4S 0A2;* [c]*Beijing Research Institute of Uranium Geology, Beijng 100029, PR China;* [d]*College of Earth Science, Chengdu University of Technology, Chengdu 610059, PR China*

(*Accepted 12 May 2011*)

Mesozoic mafic dikes in the Gan-Hang tectonic belt (GHTB) provide an opportunity to explore both the nature of their mantle source(s) and the secular evolution of the underlying Mesozoic lithospheric mantle in the region. The geochronology and primary geochemical and Sr–Nd–Pb isotopic compositions of Group 1 (middle section of GHTB) and Group 2 (the rest of the section) dolerite dikes spanning the GHTB were investigated. K–Ar ages indicate that dikes of both groups were emplaced during the Cretaceous (131–69 Ma). The dikes are doleritic in composition and are enriched in both large ion lithophile elements (LILEs; e.g. Rb, Ba, and Pb) and light rare earth elements (LREEs), with a wide range of Eu anomalies, but are depleted in high field strength elements (HFSEs; e.g. Nb, Ta, and Ti) and heavy rare earth elements (HREEs). Dikes sampled in the middle section of the GHTB (Group 1) show more pronounced REE differentiation and a greater contribution from crustal material than those from the east and west sections (Group 2) and are similar to GHTB volcanic rocks in exhibiting a slight enrichment in LREEs. The dolerites are further characterized by a wide range in $^{87}Sr/^{86}Sr_i = 0.7041–0.7110$, $^{143}Nd/^{144}Nd_i = 0.511951–0.512758$, $\varepsilon Nd_t = -10.4$ to $+5.6$, and Pb isotopic ratios ($^{206}Pb/^{204}Pb_i = 18.1–18.3$, $^{207}Pb/^{204}Pb_i \approx 15.6$, and $^{208}Pb/^{204}Pb_i = 38.2–38.7$). The dikes have undergone fractional crystallization of olivine, clinopyroxene, plagioclase, and Ti-bearing phases, except for dikes from the Anding area, which possibly experienced fractionation of plagioclase. Geochemically, all the dike samples originated from mantle sources ranging in composition from depleted to enriched that contained a component of foundered lower crust; crustal contamination during the ascent of these magmas was negligible. In the context of the late Mesozoic lithospheric extension across South China, mafic dike magmatism was likely triggered by the reactivation of deep faults, which promoted foundering of the lower crust and subsequent mantle upwelling in the GHTB.

Keywords: Cretaceous; mafic dikes; lithospheric mantle; asthenosphere; Gan-Hang tectonic belt (GHTB); South China

Introduction

Since late Mesozoic time, multiple magmatic episodes – including broadly bimodal suites of tholeiitic basalt-rhyolite and extensive swarms of mafic dikes – indicate the operation of large-scale extensional tectonics over much of SE China. Although many studies suggest that the cause of this extensional regime was lithospheric extension, controversies remain concerning the timing of events and the detailed mechanisms involved (e.g. Wang *et al*. 2003, 2005a, 2006; Zhou 2003; Mao *et al*. 2004; Hu *et al*. 2004, 2007, 2008; Wang 2004; Chen *et al*. 2005; Hua *et al*. 2005; Li and Li 2007; Li *et al*. 2007; Xu 2008). Wang *et al*. (2003) suggested that the source of Jurassic mafic rocks spanning the Chengzhou-Linwu Fault was a mixed mantle regime involving enrichment mantle I (EMI) and II (EMII) mantle sources, as well as an oceanic island basalt (OIB) component (defined by Zindler and Hart 1986). In addition, they proposed a model for the tectonic evolution of the South China Block (SCB) during the Mesozoic that invoked crustal detachment within a collisional regime prior to ~175 Ma, followed by intracontinental lithospheric extension from 175 to 80 Ma. In contrast, Zhou and Chen (2000) argued that the primary magmas responsible for igneous activity across SE China were derived from an enriched mantle source, with melting triggered by subduction of the Pacific Plate since late Mesozoic time. An additional alternative was provided by Chen and Wang (1995), who proposed that the Jiangnan Terrane was subducted beneath the Cathaysia Block during the Early Jurassic, causing deformation and partial melting of the thickened crust, which in turn led to the formation of S-type volcano-intrusive complexes.

*Corresponding author. Email: huruizhong@vip.gyig.ac.cn

ISSN 0020-6814 print/ISSN 1938-2839 online

http://dx.doi.org/10.1080/00206814.2011.588820
http://www.tandfonline.com

Models explaining the evolution of the Mesozoic lithosphere across South China can, in principle, be divided into two main perspectives. The first invokes a subduction regime, although the details of individual models vary, including an Andean-type active continental margin (Charvet *et al*. 1994), subduction of the Pacific Plate with associated underplating of basaltic magma (Zhou and Li 2000), and a low angle of subduction for the down-going Pacific slab (Li and Li 2007; Zhu *et al*. 2010). The second perspective involves intracontinental lithospheric extension and thinning, of a style commonly referred to as 'basin and range' tectonics (Gilder *et al*. 1996; Chen and Jahn 1998; Wang *et al*. 2003; Li *et al*. 2004).

To further our understanding of the Mesozoic tectonic evolution of South China it is therefore necessary to clarify which of these conflicting scenarios is responsible for Mesozoic magmatism in the region: destructive plate-margin magmatism and related extension in a back-arc type setting, or intracontinental lithospheric extension related to crustal thinning (e.g. Fan *et al*. 2003). Particular attention should be given to deep-shear faults that can undermine the integrity of the lithosphere and may consequently trigger a series of chemical processes that modify the lithosphere (Wu *et al*. 2003). However, few studies have addressed this issue; moreover, it remains unclear whether lithospheric thinning can lead to the development of deep faults or, in contrast, whether deep faults owe their existence to extension of the lithosphere (Xu *et al*. 1993; Wu *et al*. 2003; Wang *et al*. 2006, 2007).

In conjunction with the important tectonic position of the Gan-Hang tectonic belt (GHTB) in South China, the characteristics of the belt provide an excellent opportunity to resolve the controversies outlined above. Thus, in this article we present new analytical data for a representative suite of mafic dikes collected from across the GHTB. Using a combination of these results and previously published geochemical data, we examine the petrogenesis of these rocks and consider their tectonic significance with the aim of understanding the lithospheric evolution and geodynamics of South China.

Geological setting

The GHTB of the SCB is an important active tectonic-magmatic belt, as well as the site of volcanically hosted uranium, and is located at the junction of the Yangtze and Cathaysia blocks. The GHTB experienced long-term tectonic overprinting (structural, magmatic, and metamorphic) and widespread mineralization (Deng and Zhang 1989, 1997, 1999; Gilder *et al*., 1991; Goodell *et al*. 1991; Zhang 1999a, 1999b, 2004). The belt comprises several components that are delineated by three deep, large-scale fault systems: the Yongfeng–Fuzhou, Dongxiang–Guangfeng, and Jiangshan–Shaoxing. These correspond to the western, middle, and eastern sections, respectively. From west to east, the GHTB is also host to three basins: the Fuzhou–Chongren, Xinjiang, and Jinhua–Quzhou (Figure 1B).

The study area contains a package of Mesoproterozoic to Cenozoic sediments exhibiting regional differences that may be related to tectonic activity. For example, the GHTB underwent three periods of large-scale extension: lithospheric stretching in relation to Tungwu movement in Permian, which resulted in the formation of the Yongfeng–Zhuji depression; a further period of extension during the Late Jurassic, which contributed to the formation of the Gan-Hang volcanic belt; and additional extensional tectonics at the end of the Early Cretaceous, which culminated in the development of the Gan-Hang graben-bound basins. The latter two of these periods of extension were large-scale events that occurred during the Yanshanian Epoch (~195–65 Ma) and constitute the main periods of tectonic activity in the GHTB. These events also led to extensive magmatic activity, including the eruption of a bimodal basalt–rhyolite association and the emplacement of granite, gabbro, and dolerite (Goodell *et al*. 1991). As such, these igneous rocks provide an excellent opportunity to probe and systematically study both the dynamic background and the metallogenic character of the GHTB.

Mafic dikes are widely distributed across the belt, with the majority being emplaced into Jurassic–Cretaceous strata, both within and along the periphery of the 'Red Graben' Basin, named after the red colour of the strata (Figure 1). Individual dikes are commonly vertical and strike NE–SW to ENE–WSW, parallel to the main fault zones within the region. The dikes are predominantly porphyritic dolerites and extend from several kilometres to tens of kilometres along strike, with widths on the order of 10 m; there is clear evidence that they formed by the infilling of crustal fractures (e.g. mafic dikes at Jiangshan and Jinhua; Figure 2). For details on the locations of individual dikes, see Figure 1.

Analytical methods

Fresh samples were collected, taking care to avoid weathered, hydrothermally altered, or mineralized pieces. Whole-rock samples were trimmed to remove any weathered surfaces, then powdered using an agate mill. In total, 19 representative samples were analysed for major and trace elements. Major oxides were analysed with a PANalytical Axios-Advanced X-ray fluorescence (XRF) spectrometer (PANalytical B.V., Almelo, The Netherlands) at the State Key Laboratory of Ore Deposit Geochemistry (SKLODG), Institute of Geochemistry, Chinese Academy of Science (IGCAS), Guiyang, China. Fused glass discs were used for major element analysis, with an analytical precision, as determined on the Chinese National standard GSR-3, of better than 5%. Loss on ignition (LOI) determinations were obtained using 1 g of powder that was heated to 1100°C for 1 hour.

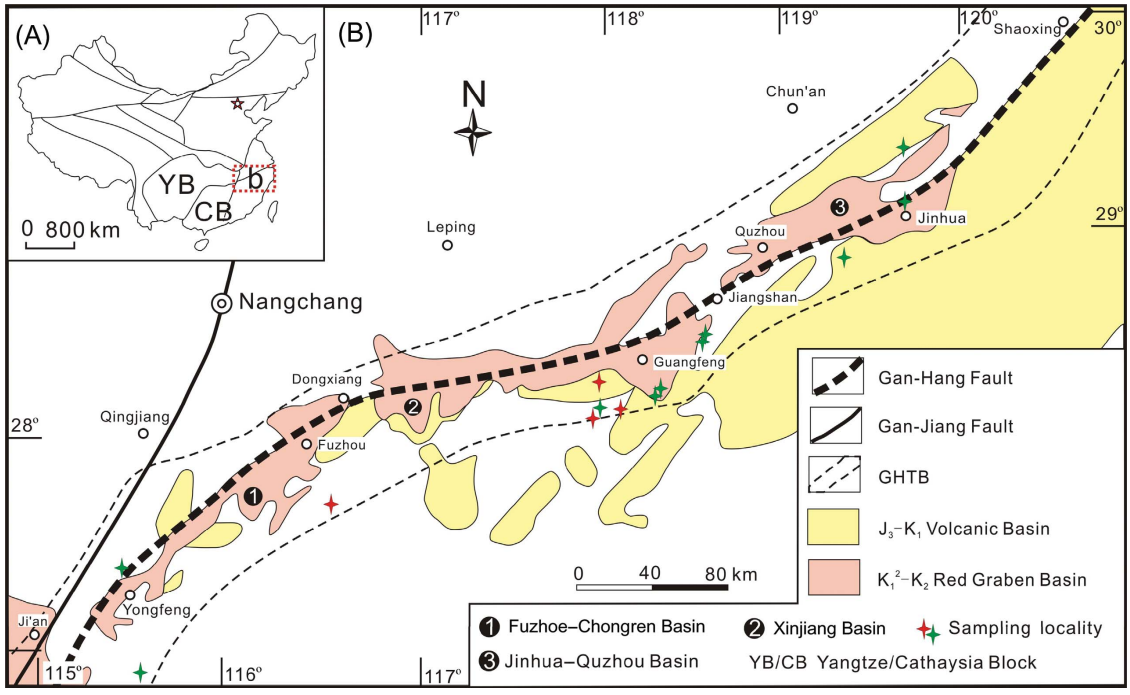

Figure 1. (A) Simplified map of China. (B) Geological map of the Gan-Hang tectonic belt (GHTB), South China and sampling localities of mafic dikes from the GHTB [green = this study, red = Xie (2003)].

Whole-rock trace element analyses, including a subset of the rare-earth elements (REEs), were carried out using a Perkin-Elmer ELAN 6000 inductively coupled plasma–mass spectrometer (ICP–MS) at IGCAS using the analytical procedures outlined by Qi *et al*. (2000). Precision and accuracy range from 5% to 10% for all elements. The results of both XRF and ICP–MS analyses are presented in Table 1.

K–Ar age determinations were carried out using an MM1200 spectrometer at the Institute of Geology, China Seismology Bureau, Beijing, China, and Beijing University, Beijing, China. Parameters used were the following: $\lambda_e = 0.581 \times 10^{-10}$ year^{-1}, $\lambda_\beta = 4.962 \times 10^{-10}$ year^{-1}, $^{40}K = 0.01167$ atom % (Steiger and Jäger 1977). Isotopic analyses for a subset of samples were performed on a MAT-262 TIMS instrument at the Institute of Geology and Geophysics, Chinese Academy of Science (IGGCAS), Beijing, China, using the analytical procedures and experimental conditions published by Liu *et al*. (2008a). The results of K–Ar dating and isotopic analysis are presented in Tables 2 and 3, respectively.

Analytical results

Petrology

Nineteen mafic dike samples from the following 10 localities were collected for the study (Figure 1B): Yongfeng (Shaxi, SX), Xiajiang (XJ), Guangfeng (GF, QB, and HSY), Jiangshan (Anding, AD; Yingpanban, YPF), Longyou (Fangtan, FT), Jinhua (Shanxiacao, SXC; Daling, DL), and Pujiang (Caoxikou, CXK). The sampled dikes are predominantly dark green dolerite and exhibit typical features (e.g. sub-ophitic plagioclase and clinopyroxene with minor olivine, orthopyroxene, and Ti-magnetite). The dikes are ~35% phenocrysts of clinopyroxene (0.2–0.5 mm) and plagioclase (0.5–1.3 mm) within a groundmass of clinopyroxene, plagioclase, magnetite, and chlorite with grain sizes of ~0.05 mm. Most plagioclase phenocrysts (mainly labradorite with An = 50–70) are euhedral, whereas clinopyroxene phenocrysts (mainly augite) are commonly subhedral. In contrast to elsewhere in the belt, samples from the middle section of the GHTB are more coarsely porphyritic (e.g. with phenocrysts of clinopyroxene of up to 1.0 mm). Figure 2 shows representative petrographic images of the samples of GHTB dikes.

Radiometric age determinations

Table 2 lists the K–Ar ages of the investigated mafic dikes. Eight samples were measured, yielding the following ages: Xiajiang (131.6 million years), Yongfeng (100.2 million years), Guangfeng (91.1–95.9 million years), Jiangshan (Anding, 69.5 million years; Yingpanban, 131.7 million years), Jinhua (123.6 million years), and Pujiang (137.4 million years). In addition to our results, Wang *et al*. (2008) reported a $^{40}Ar/^{39}Ar$ age of 90.2 million years for aplitic basalts from Luosishan (Ji'an in Jiangxi Province, southwest of GHTB), and Jiang *et al*. (2011) used SHRIMP

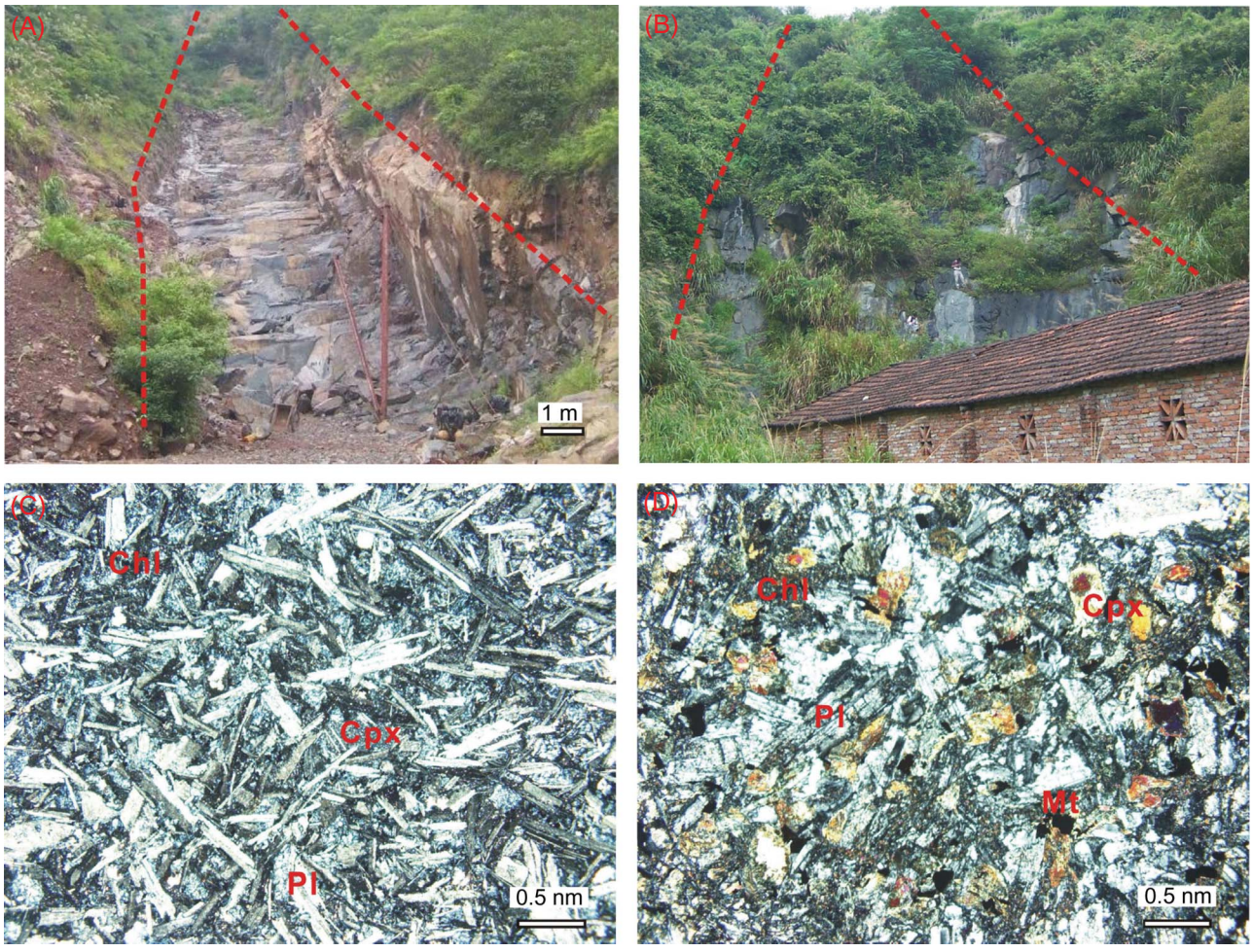

Figure 2. Field photographs of mafic dikes formed by the infilling of crustal fractures in the Anding region of Jiangshan (A) and Shanxiacao region of Jinhua (stature) (B). Representative photomicrographs of mafic dikes from Gan-Hang tectonic belt (GHTB), South China: (C) for Anding of Jiangshan; (D) for Shanxiacao of Jinhua. Cpx, clinopyroxene; Pl, plagioclase; Mt, magnetite; Chl, chlorite.

zircon U–Pb dating to show that granitic plutons and a diabasic dike to the northwest of the GHTB were emplaced in the Early Cretaceous (129–122 million years). These results are consistent with the new data presented here and, in combination with previously published ages for GHTB mafic dikes (Shao 2004; Yu *et al*. 2006), suggest that mafic dike emplacement was widespread during the Cretaceous, and thus contemporaneous with regional volcanic activity and large-scale episodes of mineralization.

Major and trace elements

Major element oxide and trace element results obtained by XRF for all samples of this study are provided in Table 1. The dolerite shows a wide range of chemical compositions (e.g. $SiO_2 = 46.7–54.7$ wt.%, $MgO = 2.7–7.9$ wt.%; Figure 3), but in a plot of Na_2O versus K_2O (not shown) the majority of samples straddle the boundary between the calc-alkaline and shoshonitic series. In a plot of total alkalis versus SiO_2 (wt.%; Figure 3A), the data span the fields of basalt, basaltic andesite, trachybasalt, and basaltic trachyandesite (Le Bas *et al.* 1986). The samples also show an alkaline to sub-alkaline character based on the classification of Irvine and Baragar (1971). A similar subdivision is apparent in a plot of Nb/Y versus Zr/TiO_2 (Figure 3B, after Winchester and Floyd 1977).

The studied mafic dikes are characterized by enrichment in light rare earth elements (LREEs) and depletion in heavy rare earth elements (HREEs), with $(La/Yb)_N$ values of 2.8–26.3 and Eu/Eu^* of 0.7–1.5 (Figure 4). In a diagram of REEs versus $(La/Yb)_N$ (Figure 5), the samples can be classified into two groups: Group 1 samples, which were mainly collected from the middle section of the GHTB, have $(La/Yb)_N$ ratios of greater than 16, whereas Group 2 samples have $(La/Yb)_N$ ratios of less than 12. Mafic dikes from Shaxi in Yongfeng show the lowest Eu/Eu^* ratios (i.e. large negative Eu anomalies), but the dikes from Anding in Jiangsha show obvious positive Eu anomalies.

In Figure 4A, the shaded region represents the range for volcanic rocks from the Jiangshan–Guangfeng area of

Table 1. Major oxides (wt.%) and trace elements (ppm) for representative mafic dikes from the GHTB, South China.

Sample no.	SX01	SX02	SX04	SX06	XJ01	GF01	GF03	QB01	HSY1	AD1	AD4	YPF1	CXK4	FT2	FT3	SXC1	SXC2	SXC4-2	DL1
Locality	Yongfeng				Xiajiang	Guangfeng				Jiangshan			Pujiang	Longyou		Jinhua			
SiO_2	53.69	51.10	53.08	53.56	52.29	49.41	51.80	49.54	50.65	50.23	50.14	49.52	54.71	50.08	49.81	47.33	49.80	46.70	47.08
TiO_2	1.19	0.93	1.18	1.18	1.04	1.87	1.94	1.97	0.91	1.28	1.32	0.98	1.11	1.32	1.19	2.28	2.14	2.78	2.82
Al_2O_3	16.59	17.02	16.48	16.67	16.33	16.51	16.78	16.96	14.52	17.45	17.76	17.72	17.86	15.34	15.51	15.66	15.30	14.99	14.07
Fe_2O_3	8.54	8.71	8.93	8.89	9.83	9.96	9.69	9.98	8.96	9.32	9.42	9.17	7.05	11.70	11.29	11.89	11.90	14.25	13.59
MnO	0.14	0.15	0.17	0.17	0.12	0.13	0.15	0.12	0.14	0.16	0.14	0.17	0.11	0.17	0.16	0.19	0.18	0.27	0.20
MgO	4.57	5.16	4.80	4.78	7.13	4.15	4.31	3.90	7.89	3.64	3.29	6.42	2.74	7.00	6.53	5.49	5.58	5.48	5.36
CaO	7.07	6.69	7.63	7.22	8.50	5.01	6.83	6.62	6.37	5.30	5.28	8.10	6.21	8.11	8.00	7.64	7.39	7.72	5.22
Na_2O	2.74	3.40	2.35	2.59	2.71	3.82	3.31	3.64	2.87	3.90	4.18	2.79	2.55	3.17	3.05	3.11	3.22	2.44	3.52
K_2O	1.98	2.94	1.78	2.01	0.45	3.19	2.60	2.85	2.72	3.56	3.10	1.71	3.39	0.90	0.83	1.10	1.27	1.46	1.03
P_2O_5	0.29	0.21	0.29	0.29	0.10	1.07	1.14	1.20	0.33	0.51	0.52	0.25	0.40	0.25	0.18	0.75	0.65	0.98	0.90
LOI	2.87	3.65	2.69	2.40	1.09	4.44	1.47	2.59	3.19	3.17	3.48	1.71	2.69	1.98	2.42	3.82	1.92	2.95	5.21
Total	99.66	99.95	99.39	99.77	99.59	99.57	100.02	99.37	98.54	98.52	98.62	98.54	98.82	100.02	98.95	99.27	99.34	100.01	99.00
Mg#	51.5	54.0	51.6	51.6	59.0	45.2	46.8	43.6	63.6	43.6	40.9	58.1	43.5	54.2	53.4	47.8	48.2	43.2	43.9
Ba	436	437	475	493	75	1912	1383	1496	1085	1414	961	597	843	277	223	675	504	592	687
Rb	72.8	192.4	62.2	67.7	22.0	61.3	51.1	46.6	152.1	131.8	119.8	57.8	80.9	23.6	24.3	29.1	51.9	50.4	18.9
Sr	312	429	327	333	219	1239	935	1250	684	629	600	679	606	457	396	559	476	547	342
Y	27.6	31.7	29.0	27.6	15.0	40.0	31.9	24.0	21.9	18.4	22.5	15.6	31.0	23.2	22.6	34.3	40.6	44.5	43.3
Zr	185.4	136.6	166.1	195.3	57.4	267.0	308.9	256.9	203.6	137.4	134.2	63.1	295.8	160.1	142.0	265.2	317.0	320.0	338.5
Nb	14.1	9.6	14.1	14.8	4.2	20.2	21.9	19.6	8.6	7.7	7.7	3.0	14.3	15.3	6.9	14.3	16.4	18.4	16.9
Th	8.3	5.5	8.2	8.4	1.2	2.4	3.2	1.8	9.5	5.2	5.1	2.7	7.4	3.6	2.8	1.8	3.8	2.4	1.8
Pb	9.8	8.5	11.8	12.1	3.4	9.6	15.9	9.2	24.3	10.7	8.1	5.7	14.3	4.5	3.9	5.9	5.3	3.4	6.1
Zn	89.9	93.2	97.9	97.1	89.1	117.0	138.1	123.8	112.7	111.3	111.6	76.2	105.1	121.9	117.2	146.1	147.5	134.9	245.1

(*Continued*).

Table 1. (Continued).

Sample no.	SX01	SX02	SX04	SX06	XJ01	GF01	GF03	QB01	HSY1	AD1	AD4	YPF1	CXK4	FT2	FT3	SXC1	SXC2	SXC4-2	DL1
Locality	Yongfeng				Xiajiang	Guangfeng				Jiangshan			Pujiang	Longyou		Jinhua			
Ni	19.2	25.2	25.3	20.9	145.9	22.7	33.4	23.2	239.3	9.2	7.2	103.2	15.2	131.7	137.7	56.8	72.0	53.9	47.6
V	190.4	196.7	199.1	197.6	128.1	180.8	194.5	179.2	150.5	185.3	178.7	211.1	151.5	169.7	167.2	230.0	206.9	264.9	264.5
Cr	39.6	66.9	60.1	46.5	246.2	53.5	67.6	58.8	416.9	19.7	18.7	212.6	36.5	238.9	240.4	143.4	102.7	71.8	103.4
Hf	4.52	3.39	4.09	4.60	1.50	5.57	6.44	5.57	5.07	3.39	3.41	1.85	7.25	3.86	3.53	5.94	7.43	7.67	7.35
Sc	21.58	24.00	23.43	22.98	17.66	16.07	16.95	14.17	19.46	22.75	21.41	22.38	15.99	22.90	22.20	25.17	24.08	27.47	30.90
Ta	0.71	0.46	0.70	0.71	0.24	0.75	0.83	0.74	0.59	0.53	0.50	0.25	0.91	1.01	0.51	0.99	1.11	1.14	1.03
Co	26.95	30.70	29.60	30.14	42.58	23.83	29.41	25.68	42.79	24.69	24.32	38.70	19.80	49.82	52.56	39.37	41.29	43.23	42.26
U	1.04	0.72	0.96	1.09	0.23	0.49	0.63	0.52	1.34	1.07	0.91	0.72	1.63	0.64	0.50	0.44	0.80	0.52	0.41
W	0.85	0.76	0.87	0.79	0.25	0.86	0.26	0.30	0.58	0.59	0.60	0.39	0.91	0.45	0.30	0.34	0.35	0.76	0.91
La	31.69	31.69	33.02	34.21	5.05	80.15	69.11	62.84	57.51	23.30	27.20	11.31	40.89	19.34	14.84	27.46	33.87	37.05	33.60
Ce	63.1	47.4	61.1	67.2	11.0	125.8	141.1	131.4	109.3	49.5	50.7	24.1	82.7	39.9	31.9	62.0	74.5	82.8	74.5
Pr	7.71	7.23	8.01	8.50	1.52	17.97	17.09	16.46	12.12	5.98	6.65	2.99	9.46	4.74	3.87	7.77	9.11	10.37	9.50
Nd	32.1	30.9	32.6	34.2	7.4	75.7	75.6	67.9	44.6	24.7	27.5	13.1	36.4	19.4	16.0	33.7	38.0	44.0	41.3
Sm	6.28	6.09	6.54	7.00	2.38	13.34	13.01	11.40	7.37	5.06	5.51	2.98	7.17	4.37	3.68	7.43	8.03	9.52	9.01
Eu	1.29	1.41	1.39	1.41	0.90	3.35	3.23	2.92	2.09	2.80	2.85	1.29	1.94	1.39	1.22	2.49	2.44	3.11	3.07
Gd	5.85	6.42	6.29	6.15	2.80	11.20	10.40	8.65	7.71	6.33	6.06	3.72	7.95	5.22	4.61	8.61	9.38	11.18	10.69
Tb	0.81	0.88	0.83	0.86	0.44	1.32	1.25	0.99	0.79	0.67	0.73	0.49	0.97	0.74	0.68	1.14	1.29	1.46	1.40
Dy	4.86	5.30	5.11	5.14	2.85	6.58	6.51	5.14	4.42	3.78	4.19	2.93	5.92	4.55	4.21	6.80	7.76	8.56	8.41
Ho	0.95	1.02	1.00	0.99	0.53	1.21	1.16	0.85	0.82	0.73	0.79	0.60	1.16	0.90	0.85	1.34	1.54	1.69	1.65
Er	2.86	2.95	2.82	2.76	1.53	3.04	3.22	2.40	2.41	1.97	2.16	1.69	3.35	2.48	2.41	3.72	4.34	4.65	4.61
Tm	0.40	0.39	0.40	0.39	0.20	0.38	0.44	0.29	0.32	0.27	0.29	0.24	0.48	0.34	0.34	0.51	0.62	0.64	0.63
Yb	2.52	2.51	2.44	2.55	1.32	2.31	2.84	1.86	2.07	1.68	1.85	1.58	3.12	2.20	2.23	3.30	3.98	4.10	3.98
Lu	0.38	0.38	0.37	0.39	0.19	0.34	0.38	0.28	0.30	0.25	0.27	0.24	0.47	0.33	0.33	0.48	0.59	0.61	0.59
ΣREE	160.74	144.50	161.86	171.77	38.06	342.76	345.33	313.30	251.80	127.03	136.74	67.21	201.96	105.92	87.18	166.74	195.48	219.70	202.89
$(La/Yb)_N$	9.0	9.1	9.7	9.6	2.8	24.9	17.4	24.2	19.9	9.9	10.5	5.1	9.4	6.3	4.8	6.0	6.1	6.5	6.0
Eu/Eu*	0.7	0.7	0.7	0.7	1.1	0.8	0.8	0.9	0.8	1.5	1.5	1.2	0.8	0.9	0.9	1.0	0.9	0.9	1.0

Note: LOI, loss on ignition. $Mg\# = 100^{*}Mg/(Mg + \Sigma Fe)$ atomic ratio. $(La/Yb)_N = La_N/Yb_N$, normalized to the primitive mantle of Sun and McDonald (1989).

Table 2. K–Ar ages of mafic dikes from the GHTB, South China.

Locality	Sample	K (wt.%)	^{40}Ar (mol/g)	^{40}Ar$_a$ (%)	Apparent age (Ma) ± 1σ	Reference
Jiangshan	YPF1	1.43	3.38E-10	54.39	131.74 ± 11.11	This study
Jiangshan	AD1	3.56	4.37E-10	40.25	69.50 ± 3.13	This study
Qianshan	HSY1	2.52	6.18E-10	73.65	136.24 ± 6.64	This study
Pujiang	CXK4	2.98	7.37E-10	63.04	137.42 ± 9.49	This study
Jinhua	SXC2	2.55	5.65E-10	55.33	123.55 ± 13.80	This study
Guangfeng	GF03	2.29	3.71E-10	96.39	91.14 ± 1.75	This study
Guangfeng	QB01	2.42	4.14E-10	94.16	95.92 ± 1.88	This study
Xiajiang	XJ01	0.40	9.47E-11	69.00	131.6 ± 4.1	This study
Qianshan	6403	2.35	5.92E-10	83.22	139.8 ± 2.8	Xie (2003)
Qianshan	SLX5	1.64	3.48E-10	85.03	118.5 ± 2.0	Xie (2003)
Maopai	MP4	1.54	2.99E-10	82.06	108.5 ± 1.7	Xie (2003)
Maopai	MG4	1.13	1.96E-10	87.50	97.3 ± 1.7	Xie (2003)
Yongfeng	YFX2	1.66	2.97E-10	84.82	100.2 ± 1.6	Xie (2003)
Qianshan	SLX2	2.37	4.47E-10	88.17	105.7 ± 1.6	Xie (2003)
Qianshan	CF1	1.68	3.32E-10	87.11	110.4 ± 2.1	Xie (2003)

Parameters for ^{40}K: $\lambda_e = 0.581 \times 10^{-10}$ year^{-1}, $\lambda_\beta = 4.962 \times 10^{-10}$year^{-1}, ^{40}K = 0.01167 atom% (Steiger and Jäger 1977).

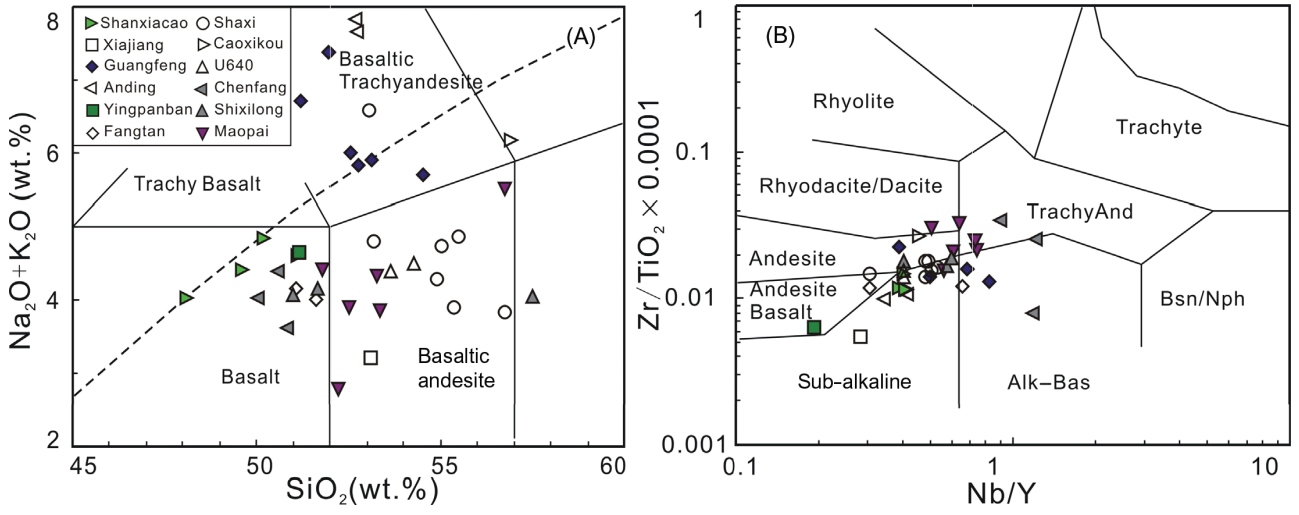

Figure 3. (A) Total alkalis ($K_2O + Na_2O$) versus SiO_2 diagram, showing the range in rock types for mafic dikes from the Gan-Hang tectonic belt (GHTB), South China (reference fields are from Le Bas *et al.* 1986); the division between alkaline and sub-alkaline is after Irvine and Baragar (1971). (B) Zr/TiO_2 versus Nb/Y diagram for the studied mafic dikes (reference field from Winchester and Floyd 1977).

South China (Yu *et al*. 2006). Group 1 samples are similar in terms of total REE abundances to these volcanic rocks and also display a slight enrichment in LREEs. In contrast, Group 2 samples display weaker slope in the REE trend, less enrichment in the LREE than that present in the Jiangshan-Guangfeng volcanic rocks. Primitive-mantle-normalized trace element diagrams (Figure 4C and 4D) show that GHTB mafic dikes are enriched in large ion lithophile elements (LILEs; i.e. Rb, Ba, Pb, and Th), but depleted in Sr and high field strength elements (HFSEs; i.e. Nb, Ta, P, and Ti). These characteristics are shared by the Jiangshan-Guangfeng volcanic rocks, although the latter have even higher abundances of Pb.

Ni, Cr, and Co concentrations of the studied mafic dikes range from 7.2 to 239 ppm, 18.7 to 417 ppm, and 19.8 to 52.6 ppm, respectively; rocks from Yingpanban, Xiajiang, Fangtan, and Huangshayuan have relatively high contents of Ni and Cr. All samples show positive correlations of MgO versus Ca, Cr, and Ni, and negative correlations of MgO versus SiO_2, Al_2O_3, and TiO_2; MgO shows no correlation with Sr or Th (Figure 6).

Sr–Nd–Pb isotopic compositions

Table 3 lists the Sr, Nd, and Pb isotopic compositions of the investigated samples. The dikes exhibit a wide range in $^{87}Sr/^{86}Sr_i$, $^{143}Nd/^{144}Nd_i$, and εNd_t values (from 0.704098 to 0.711026, 0.511951 to 0.512758, and –10.4 to +5.6, respectively). For comparison, Figure 7 shows the isotopic results of this study along with data for other mafic rocks

Table 3. Sr, Nd, and Pb isotopic ratios of mafic dikes from the GHTB, South China.

Sample	$^{87}Rb/^{86}Sr$	$^{87}Sr/^{86}Sr$	$\pm 2\delta$	$^{87}Sr/^{86}Sr_i$	$^{147}Sm/^{144}Nd$	$^{143}Nd/^{144}Nd$	$\pm 2\delta$	$^{143}Nd/^{144}Nd_i$	εNd_t	$^{206}Pb/^{204}Pb$	$^{207}Pb/^{204}Pb$	$^{208}Pb/^{204}Pb$	$^{206}Pb/^{204}Pb_i$	$^{207}Pb/^{204}Pb_i$	$^{208}Pb/^{204}Pb_i$
GF03	0.1579	0.708769	14	0.708566	0.1040	0.512235	14	0.512173	–6.8	18.320	15.624	38.739	18.284	15.622	38.679
XJ01	0.2905	0.704635	13	0.704098	0.1943	0.512925	14	0.512758	5.6	18.248	15.595	38.595	18.159	15.591	38.447
QB01	0.1080	0.707876	10	0.707730	0.1015	0.512327	11	0.512263	–4.9	18.187	15.601	38.606	18.133	15.598	38.546
SXC2	0.3151	0.707031	13	0.706480	0.1278	0.512435	15	0.512331	–2.9	18.310	15.553	38.500	18.125	15.544	38.210
YPF1	0.2463	0.706875	11	0.706416	0.1381	0.512471	16	0.512352	–2.3	18.429	15.567	38.511	18.264	15.559	38.308
CXK4	0.3863	0.708503	11	0.707756	0.1193	0.512254	15	0.512147	–6.1	18.380	15.592	38.664	18.225	15.584	38.433
HSY1	0.6441	0.712108	13	0.711026	0.1000	0.512029	14	0.511951	–10.4	17.635	15.536	37.989	17.571	15.533	37.841
AD1	0.6066	0.709287	13	0.708688	0.1237	0.512301	14	0.512244	–5.9	18.271	15.614	38.836	18.201	15.611	38.725

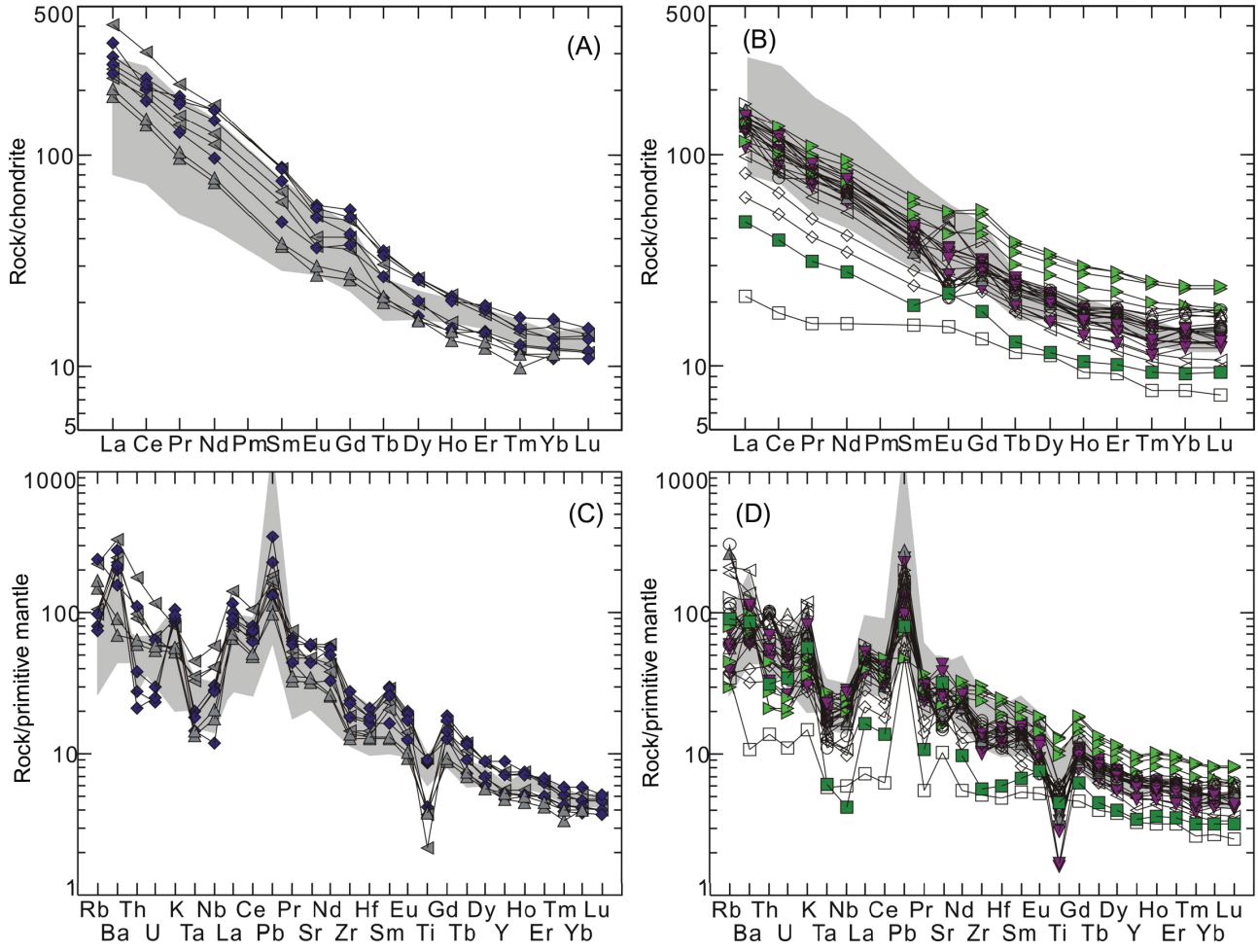

Figure 4. Chondrite-normalized rare earth element (REE) patterns and primitive-mantle-normalized multi-element diagrams of mafic dikes from the GHTB, South China: (A) and (C) are for Group 1 dikes; (B) and (D) are for Group 2. Normalizing values are after Sun and McDonough (1989). The shaded area represents data from a volcano from the Jiangshan-Guangfeng area (middle part of the GHTB), after Yu *et al*. (2006).

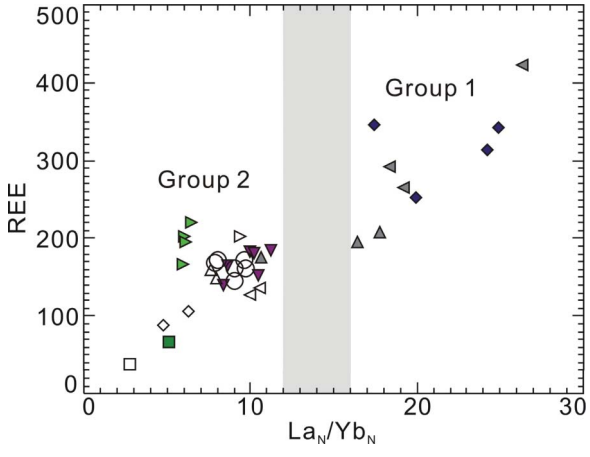

Figure 5. Rare earth element (REE) versus $(La/Yb)_N$ diagram for mafic dikes from the Gan-Hang tectonic belt (GHTB), South China. Normalization data are after Sun and McDonough (1989). Symbols are as in Figure 3.

from across South China and Shandong. When combined with isotopic data from other parts of the GHTB (yellow area in Figure 7), the dolerites form an approximately linear trend towards an EMII composition. Moving southwards across South China (i.e. from Ganbei to Gannan and Yuebei; see Figure 7), there is a characteristic counterclockwise rotation in the distribution of samples from a given region in $^{87}Sr/^{86}Sr_i$ versus εNd_t space. Regionally, samples from the central GHTB (i.e. Guangfeng) generally have lower Nd and higher Sr isotopic compositions than other samples. Samples older than ~130 million years display lower Nd and higher Sr isotopic ratios than those younger than ~130 million years. However, the Xiajiang dike, which has an emplacement age of 140 million years, has the highest Nd isotopic ratio.

The Pb isotopic ratios of the studied dikes are characterized by $^{206}Pb/^{204}Pb_i = 18.1–18.3$, $^{207}Pb/^{204}Pb_i \approx 15.6$, and $^{208}Pb/^{204}Pb_i = 38.2–38.7$, with the exception of

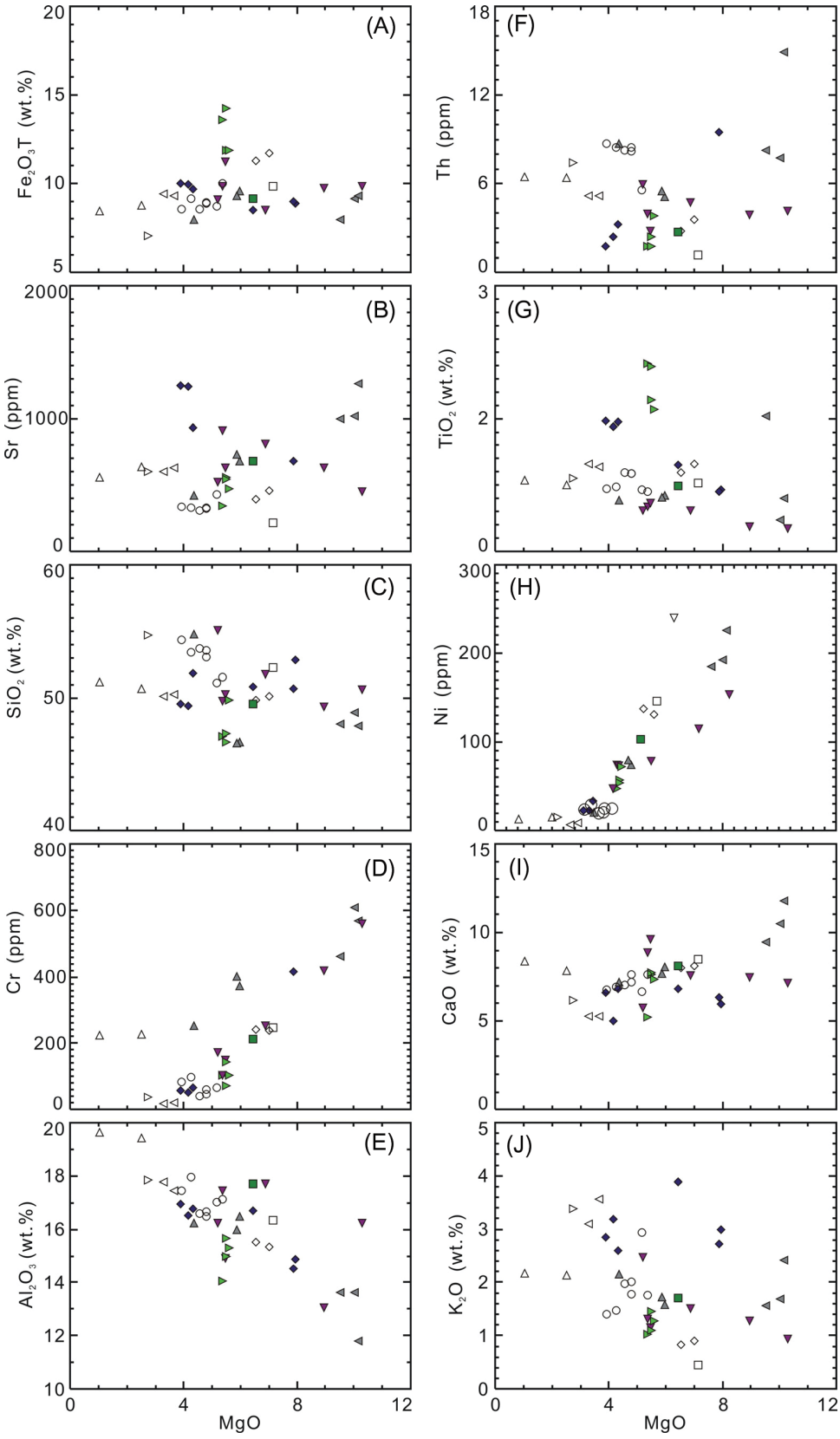

Figure 6. Variation diagrams for major oxides and trace elements versus MgO contents for mafic dikes from the Gan-Hang tectonic belt (GHTB), South China. (A) Fe_2O_3T vs MgO, (B) Sr vs MgO, (C) SiO_2 vs MgO, (E) Al_2O_3 vs MgO, (F) Th vs. MgO, (G) TiO_2 vs MgO, (H) Ni vs MgO, (I) CaO vs MgO, (J) K_2 vs MgO. Symbols are as in Figure 3.

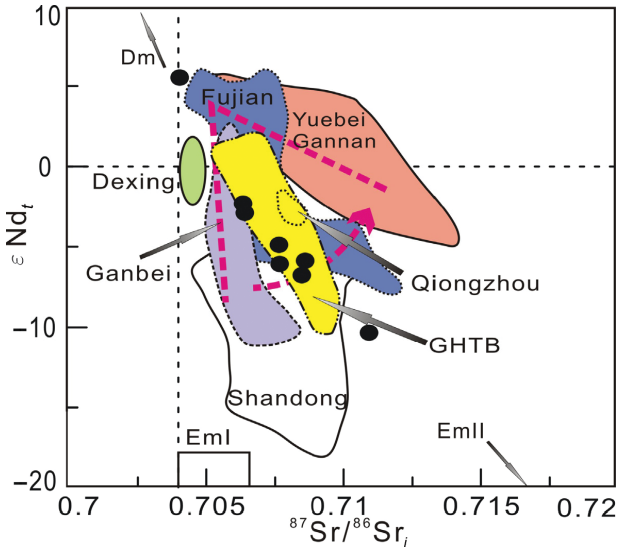

Figure 7. Initial $(^{87}Sr/^{86}Sr)_i$ versus εNd_t value for mafic rocks from the Gan-Hang tectonic belt (GHTB), South China. The shaded fields represent data from the following sources: Fujian data are from Zhou and Chen (2001), Zhao (2004), and Mao *et al*. (2006); Yuebei and Gannan data are from Li *et al*. (1990, 1997, 1998) and Xie (2003); Qiongzhou data are from Ge *et al*. (2003); Ganhang data are from Chen and Wang (1995), Xie (2003), and Yu *et al*. (2004); Ganbei data are from Xie (2003); Shandong data are from Liu (2004, 2008a,b) and Yan and Chen (2007); Dexing data are from Wang *et al*. (2004).

sample HSY1 (Figure 8; Table 3). As such, they are significantly different from those of lower Yangtze lithospheric mantle (Yan *et al*. 2003), but nearly identical to those of Jiangxi mafic dikes (Xie *et al*. 2006; Figure 8A and 8B). Furthermore, the dikes from the study region are different to Pacific mid-ocean ridge basalt (MORB) and to Southern Fujian mafic dike rocks, which are believed to be related to plate subduction (Zhao *et al*. 2007).

Discussion

Fractional crystallization

Fractional crystallization generally plays an important role in magmatic evolution (Hawkesworth *et al*. 2000). The low MgO contents and Mg numbers (Mg#) of the GHTB mafic dikes, together with the presence of clinopyroxene and olivine phenocrysts, indicate fractionation of both minerals during dike evolution. In Harker diagrams (Figure 6), MgO correlates positively with Ni, Cr, and CaO, and negatively with SiO_2, Al_2O_3, and TiO_2. These trends indicate the fractionation of olivine, clinopyroxene, plagioclase, and Ti-bearing phases (e.g. rutile, ilmenite, and titanite) during magma evolution. In addition, the removal of Ti–Fe oxides from the melt might account for the negative Nb, Ta, and Ti anomalies observed in primitive-mantle-normalized multi-element diagrams (Figure 4). Both negative and positive Eu anomalies (i.e. $Eu/Eu^* = 0.7–1.5$) indicate that significant degrees of both fractionation and accumulation of plagioclase occurred.

Crustal contamination

Crustal contamination often has a significant impact during magma emplacement and its effects must be evaluated carefully. The mafic dikes of this study are believed to have been emplaced in an extensional environment, which may have resulted in a degree of crustal contamination during ascent (Mohr 1987). Mafic rocks from the

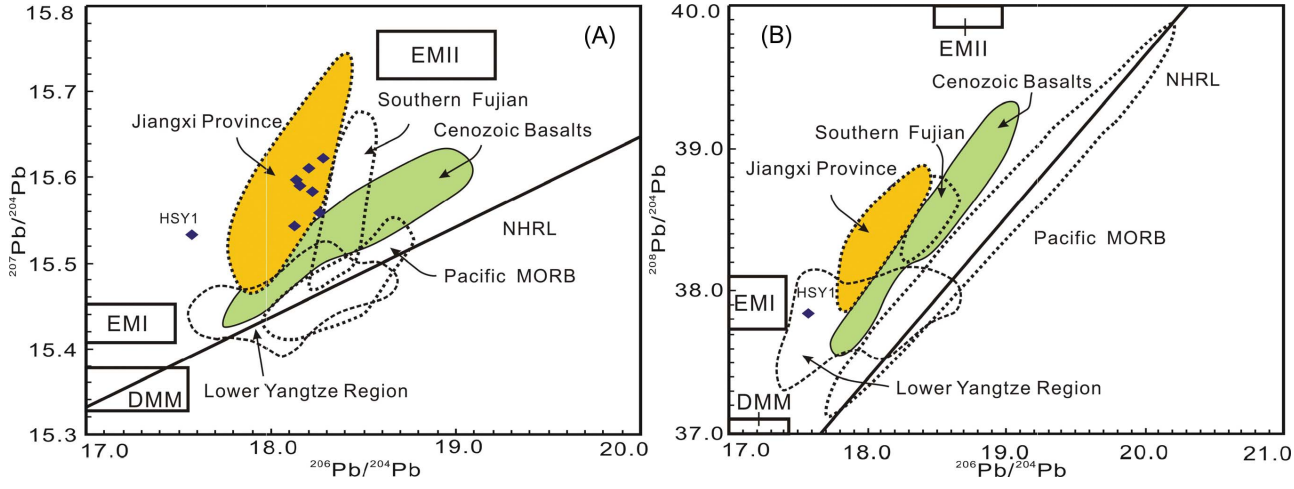

Figure 8. Pb isotopic ratios of mafic dikes from the Gan-Hang tectonic belt (GHTB), South China. (A) $^{207}Pb/^{204}Pb$ vs 206Pb/204Pb, (B) $^{208}Pb/^{204}Pb$ vs $^{206}Pb/^{204}Pb$. Fields for DMM, enrichment mantle I (EMI), and II are after Zindler and Hart (1986); Cenozoic basalts from East China and Pacific mid-ocean ridge basalt (MORB) are after Tu *et al*. (1991) and Zou *et al*. (2000), respectively; lower Yangtze data are from Yan *et al*. (2003); data for mafic rocks from Southern Fujian and Jiangxi are from Zhao *et al*. (2007) and Xie *et al*. (2006), respectively; the NHRL (Northern Hemisphere Reference Line) is after Hart (1984).

GHTB mostly display negative εNd_t values, accompanied by higher $^{87}Sr/^{86}Sr_i$ values, which could indicate contamination by crustal materials (Liu *et al*. 2009a). However, their low concentrations of Th, U, and Pb (1.18–14.9, 0.233–2.42, and 3.38–24.3 ppm, respectively) relative to published data for the upper–middle crust (Rb = 84 ppm, Th = 10.5 ppm, U = 2.7 ppm, and Pb = 20 ppm; Rudnick and Gao 2003) suggest that they were not significantly affected by upper–middle crustal contamination (Taylor and McLennan 1985). Although it is possible that lower crustal contamination occurred, available isotopic data (i.e. $^{87}Sr/^{86}Sr_i$ and εNd_t) preclude significant crustal contamination in the development of these dikes, and the geochemical and isotopic signatures may simply reflect derivation from an enriched mantle source. There is a strong correlation between La/Sm and La concentration (not shown) in the dolerites, suggesting that these dikes are mainly the products of partial melting of mantle material (Cocherie 1986).

Nature of the mantle source

Mafic dikes are believed to have originated directly from the mantle (Liu *et al*. 2006, 2008a,b, 2009a). The Sr–Nd isotopic compositions of mafic dikes across the GHTB vary greatly (Table 3; Figure 7) and show a clear linear distribution between depleted mantle (DM) and EMII mantle sources, indicating a trend from an enriched lithospheric mantle source to a depleted asthenospheric mantle source. The εNd_t and εHf_t values (*in situ* zircon analysis) of a diabasic dike from northwest of the GHTB are +0.9 and –7.1, respectively (Jiang *et al.* 2011), suggesting that it was derived from a portion of asthenospheric mantle wedge that was metasomatized by melts derived from subducted sediment. In addition, the characteristic counter-clockwise rotation of trends in $^{87}Sr/^{86}Sr_i$ versus εNd_t (Figure 7) could indicate a transition from an EMI source for the Yangtze Block to an EMII-type mantle source for the southern Cathaysia Block. If so, the mafic dikes of this study may represent an interaction between the two blocks, which meet at this tectonic division of the SCB.

A diagram of Ba/Nb versus La/Nb (Figure 9) shows a large spread in elemental ratios, with a predominantly linear distribution. This differs from most intra-plate volcanic rocks (e.g. N-MORB, OIB, alkali basalt, and kimberlite), which have La/Nb ratios of 0.5–2.5 and much lower Ba/Nb ratios of 1–20 (Figure 9). These differences suggest that continental materials (e.g. granitoids, granulites, and/or sedimentary rocks) were involved in the development of the mantle-derived partial melts that formed the GHTB mafic dikes (Jahn *et al*. 1999). As such, the heterogeneity of the mantle source(s) is likely to relate to the proportion of continental material incorporated into the source during melting. Garnet has a high partition coefficient for Y ($D_{garnet/melt}$ = 4–11) relative to Zr ($D_{garnet/melt}$ = 0.4–0.7;

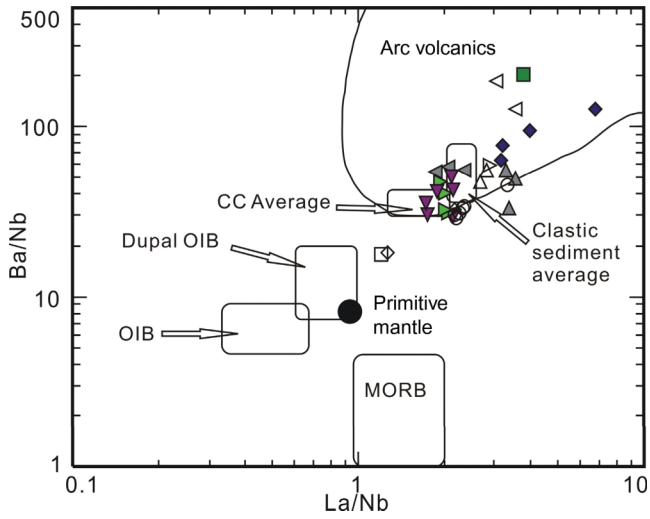

Figure 9. Ba/Nb versus La/Nb diagram for mafic dikes from the Gan-Hang tectonic belt (GHTB), South China. The basic diagram is after Jahn *et al*. (1999), with the following data sources: Primitive Mantle (PM) (Sun and McDonough 1989), continental crust average (Taylor and McLennan 1985; Condie 1993), clastic sediment average (Condie 1993), mid-ocean ridge basalt (MORB), oceanic island basalt (OIB), and Dupal OIB (Le Roux 1986).

Jenner *et al*. 1993), and residual garnet in the source can affect the Y contents of the products of melting. In a plot of Zr/Y versus Y (not shown), the mafic dikes from Maopai, Guangfeng, Shixilong, Yongfeng, and Jiangshan display a very strong negative correlation, suggesting that the source may be rich in garnet.

Because melts from the asthenosphere are susceptible to modification of their Pb isotopic composition within the lithosphere, Pb isotopic data are important in the identification of basement as either a source or a contaminant. The majority of Pb isotopic data for mafic dikes of this study are consistent with the presence of crustal material from the Cathaysia Block in the source of these magmas. Previous tectonic investigations in the study area suggest that South China is the result of a collision between the Yangtze and Cathaysia blocks during the Indosinian Orogeny, as indicated by Pb isotopic data (e.g. Chen 1999; Carter *et al*. 2001; Li *et al*. 2003, 2004; Wang and Shen 2003). In addition, the range in Pb isotopic data for mafic dikes from the GHTB differs from that of Cenozoic basalts from across South China, which are considered to have been derived from either asthenosphere or juvenile lithosphere (Chung *et al*. 1994). This difference implies that crustal material (especially old crust) was incorporated into the source of the GHTB dikes, resulting in mantle enrichment during this late Mesozoic collisional event. Therefore, our Pb isotopic data record the resulting evolutionary trend of the lithospheric mantle below the Cathaysia Block.

It has been shown above that crustal contamination (from the upper–middle crust in particular) is absent or

negligible in the investigated dike rocks. Moreover, it is thought that old upper crust is absent in the Cathaysia Block (Chen *et al*. 1999). Hence, the GHTB mafic dikes were most probably derived from the partial melts of an enriched lithospheric mantle source, which was slightly modified by melts from the lower crust beneath the Cathaysia Block.

Petrogenetic model

Zirconium and Y can maintain a degree of stability during magmatic evolution, which makes them very effective discriminators in determining palaeo-tectonic environments. In a plot of Zr/Y versus Zr (Figure 10, after Pearce and Norry 1979), the studied GHTB mafic dikes fall within the field of within-plate basalts.

The above analysis, combined with our Pb isotopic data, shows that crustal material from the Cathaysia Block was added to the source of the studied dike rocks. There are several possible models to account for the incorporation of crustal material into the mantle source of the GHTB mafic magmas, including collision between or subduction of the Yangtze and Cathaysia blocks during the Mesozoic (Chen and Wang 1995), subduction of the palaeo-Pacific Plate (Li and Zhou 2001; Li and Li 2007), thermo-chemical erosion, and delamination or foundering of lower crust (Wang *et al*. 2006). Each of these is discussed in turn below.

First, we focus on the model of collision between the Yangtze and Cathaysia blocks. The Indosinian Collision occurred mainly within the Qinling–Dabie Belt and the Song–Ma Belt in SE Asia (Carter *et al*. 2001), meaning that South China, which was sandwiched between the two, was not part of the main collisional belt. Furthermore, because magmatic activity occurred mainly during the late Yanshanian, it is possible that the Indosinian Collision did not directly affect magmatic activity in the study area. Thus, in the absence of further evidence in support of this interpretation, we do not support the collisional model as an explanation for the occurrence of the mafic rocks of this study.

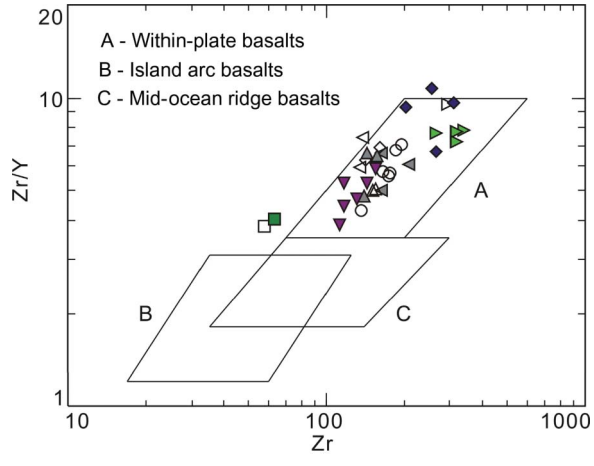

Figure 10. Zr/Y versus Zr diagram for mafic dikes from the Gan-Hang tectonic belt (GHTB), South China. Symbols are as in Figure 3. Data sources for A, B, and C are after Pearce and Norry (1979).

For the model of subduction between the Yangtze and Cathaysia blocks during the Mesozoic, Chen and Wang (1995) considered that the direction of subduction was from the Yangtze Block to the Cathaysia Block. This is, however, inconsistent with the characteristics of our Pb isotopic data. Alternatively, it has been proposed that subduction of the palaeo-Pacific (Izanagi) Plate (Zhou and Li 2000) could account for the petrogenesis of Mesozoic magmatism across South China. The angle of palaeo-Pacific Plate subduction beneath South China is thought to have increased from a very low angle to a medium angle, thereby influencing areas inland of the Hunan migration to the coasts of Fujian and Taiwan. Plate convergence thus provided the conditions necessary for intense magmatic activity across South China during the Mesozoic. It should be noted, however, that some studies have postulated that subduction of the palaeo-Pacific Plate was actually north–northeastward during the late Mesozoic (Maruyama and Send 1986; Kimura *et al*. 1990; Ratschbacher *et al*. 2000), which would provide little opportunity for the development of back-arc extensional tectonics in the region. In addition, large areas of SE China host granites and volcanic rocks which occur parallel to the shoreline (Zhou *et al*. 2006), as well as along the border region between the Yangtze and Cathaysia blocks, with their distribution controlled by faults. Hence, based on the distribution of igneous rock, there is no clear evidence that subduction of the palaeo-Pacific Plate played a role in the development of the GHTB magmas.

In considering thermo-chemical erosion and delamination in the genesis of the mafic GHTB magmas, differences between the models should be carefully considered. Menzies *et al*. (2007) examined these two models in detail, which they term ‘top-down’ (rapid delamination) and ‘bottom-up’ (a more protracted period of thermo-chemical erosion lasting ca. 100 Ma). Earlier studies had shown that thermo-chemical erosion in the axis of a deep fault will be associated with a greater degree of partial melting, that is, the addition of lithospheric mantle (Chung *et al*. 1994, 1995). In contrast, rapid delamination will cause fast upwelling of asthenospheric mantle, meaning that any melts and magmatic rocks formed during this period will exhibit asthenospheric characteristics. Given the geochemical traits of the mafic dikes of this study (i.e. early mafic rocks that display partial depleted mantle εNd_t values; unpublished data), we are more inclined to support only small-scale delamination. However, we cannot rule out thermo-chemical erosion following delamination, because it is not easy to distinguish between the two processes in detail. In addition, a dike from Xiajiang has

Table 4. Mixed end-member compositions.

	DMM	PSM	AOC-fluid	MORB-melt	PREC
$^{87}Sr/^{86}Sr_i$	0.7025	0.7090	0.7045	0.7045	0.7220
Sr (ppm)	14.8	3145	558	1509	95
$^{143}Nd/^{144}Nd_i$	0.51315	0.51238	0.51315	0.51315	0.51150
Nd (ppm)	1.24	1208	0.148	108	20

DMM from Ishizuka *et al*. (2003); PSM (Pacific sediment melts) from Plank and Langmuir (1998); AOC-fluid (Altered Oceanic Crust fluid) was estimated through balance fractionation between 2% fluid and oceanic crust (Ishizuka *et al*. 2003), isotopic composition from Staudigel *et al*. (1996); MORB-melt (melts of mafic plate subduction) from White *et al*. (1987); PREC (Precambrian metamorphic rock) from Hu and Zhang (1998), Xie (1996), Ma and Xiang (1993).

a relatively low trace element pattern and positive εNd_t, strongly supporting the proposed delamination model.

It has been proposed that foundering of lower continental crust into an underlying convecting mantle could play a role in the development of mantle plumes, in the evolution of continental crust, and in the formation of chemical heterogeneities within the mantle (Arndt and Goldstein 1989; Kay and Kay 1991; Rudnick and Fountain 1995; Jull and Kelemen 2001; Escrig *et al*. 2004; Gao *et al*. 2004, 2008; Elkins-Tanton 2005; Lustrino 2005; Anderson 2006; Liu *et al*. 2008a,b, 2009b, 2010, 2011). Because we prefer a delamination model for the origin of the GHTB mafic magmas, the following section focuses on the scale of the delamination considered to be responsible for the generation of the lithospheric mantle source that produced the GHTB mafic magmas.

As discussed above, delamination occurs mainly in foundered lower crust. Based on the regional geology of South China, Precambrian metamorphic rock (PREC) is considered to be a likely candidate, and because of the highly radiogenic $^{87}Sr/^{86}Sr_i$ composition of ancient crust, isotopic ratios can be an important constraining factor in testing the delamination model. Previous studies have demonstrated that Precambrian metamorphic rocks across South China exhibit a wide range in isotopic compositions ($^{87}Sr/^{86}Sr_i = 0.711–0.732$, $^{143}Nd/^{144}Nd_i = 0.5121$; Ma and Xiang 1993; Hu and Zhang 1998). Because of the active nature of Sr relative to Nd, and the larger age corrections required, we chose an initial Sr ratio of 0.7220 for Precambrian metamorphic basement (see Table 4). Figure 11 shows that the studied GHTB mafic dikes fall on a mixing curve between depleted MORB mantle (DMM) and PREC, in a range corresponding to 1–10% of the PREC component, and that there was a greater involvement of crustal material in Group 1 dikes than in Group 2. Figure 11 also shows that the data form of GHTB is different from Fujian so that its mafic rocks are thought to be related with subduction of the Pacific Plate (Zhao *et al*. 2004, 2007).

The long-term geological evolution of the GHTB is conducive to the involvement of metamorphic basement. During the early Neoproterozoic, following the closure of the Palaeo-Huanan Ocean, the Cathaysia Block collided with the Yangtze Block to form part of the Rodinia

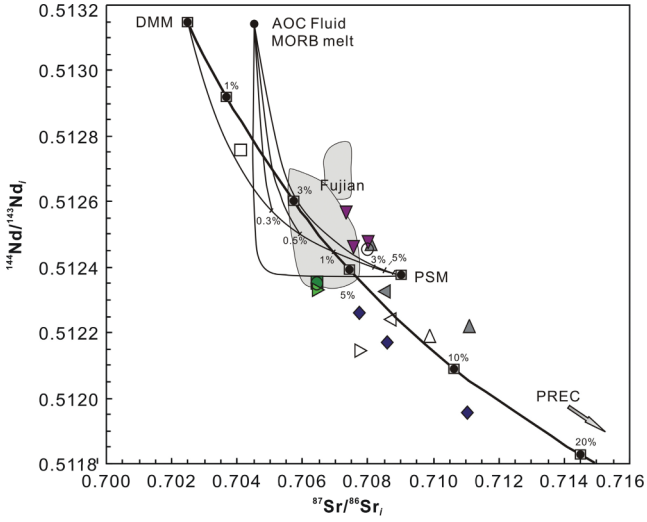

Figure 11. $(^{87}Sr/^{86}Sr)_i$ versus $(^{143}Nd/^{144}Nd)_i$ diagram of mafic dikes from the Gan-Hang tectonic belt (GHTB), South China. Symbols are as in Figure 3. Further information is listed in Table 4.

supercontinent (Li *et al*. 2002). This was followed by the breakup of Rodinia, during which time the Cathaysian Block split into several sub-blocks, with rifts or sea channels developing between them (Shu 2006). Subsequently, intense collisions occurred along the Jiangshan–Shaoxing Fault as the GHTB prototype (Zhou and Zhu 1993), which led to the incorporation of old crustal material into mantle (resulting in mantle enrichment). As such, the regional geochemical variations observed across SE China may reflect differences between individual tectonic basements (Deng *et al*. 2002).

Tectonic processes and their significance in the GHTB

Many researchers have noted the lithospheric thinning and large-scale late Mesozoic mineralization that occurred across South China (Hua *et al*. 2005; Hu *et al*. 2008), but magmatic activity and tectonic constraints are still largely overlooked in large-scale tectonic reconstructions of the South China area. In fact, this study area may represent an ancient rift zone, as geochemical characteristics support a rifting origin (e.g. Na_2O/K_2O ratios range from 0.45 to

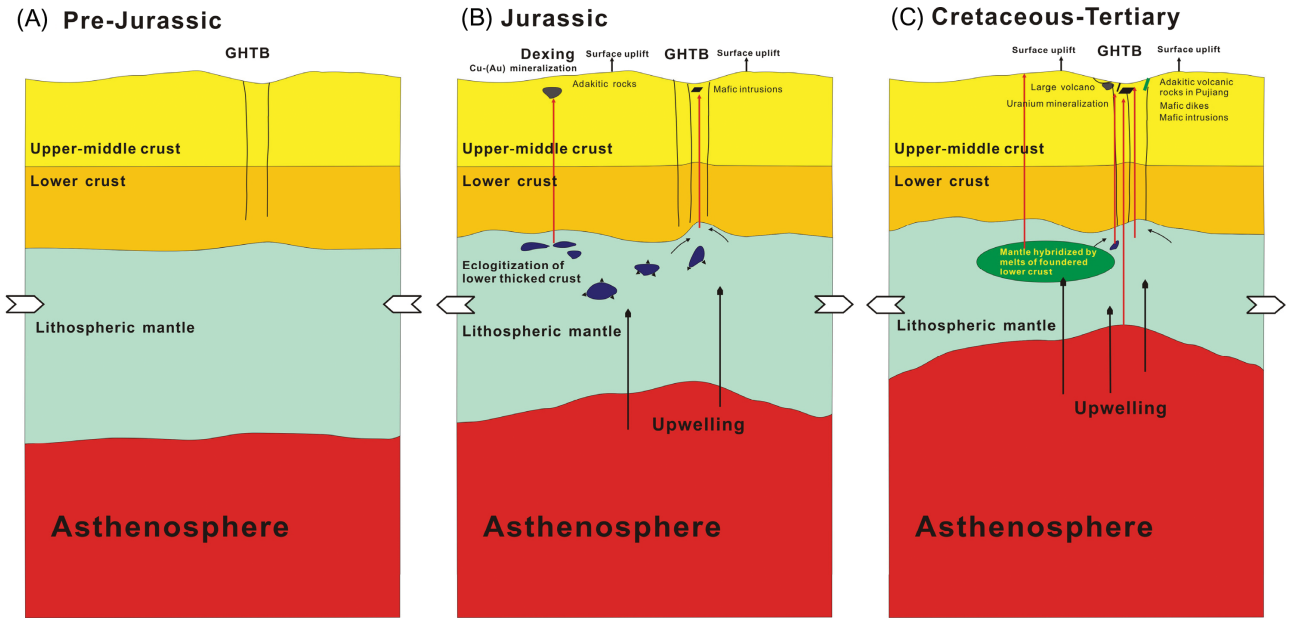

Figure 12. Proposed model for the formation of the Gan-Hang tectonic belt (GHTB) mafic dikes and other rocks via progressive hybridism of foundered lower crust since the pre-Jurassic in the South China area. (A) Collision of the Yangtze and Cathaysia blocks during the Indosinian Orogeny caused crustal thickening. (B) Due to its higher density (relative to peridotite), eclogitized thickened lower crust foundered into the lithospheric mantle in the Early Jurassic, inducing the upwelling of hot asthenosphere. During this time, adakitic rocks and Cu–(Au) mineralization formed at Dexing, and mafic dikes of the GHTB were emplaced (Wang *et al*. 2006). (C) Decompressional melting of the hybridized lithospheric mantle produced 'pristine' basaltic melts, followed by extensive volcanism throughout the area, uranium mineralization, and the formation of mafic dikes. In addition, partial melting of residual ecologitic lower crust produced the younger adakitic volcanic rocks of Pujiang (135–126 Ma; Qin *et al*. 2006).

6.05, and areas with elevated Na_2O/K_2O ratios are located in the axis of the belt). Thompson and Gibson (1994) confirmed that a mafic, ultrapotassic component that provides a distinctive input to magmas from a lithospheric source appears to be largely feasible at temperatures well below the dry solidus of subcontinental lithospheric mantle (SCLM). This would promote melting and magma production in the flanks of the rift zone, due to localized upwelling of Na-rich asthenosphere along the rift axis, which in turn causes melting at shallow depths. Hence, the magmatic activity would have been affected by both asthenospheric and lithospheric mantle along the axis and the flanks of the rift zone. This relationship is clearly reflected in εNd_t values and in the typical elemental and isotopic ratios of the studied mafic rocks (i.e. Ba/Nb = 17.8–199.1 and La/Ta = 19.1–106.9, as compared with primitive mantle values of Ba/Nb = 9.8 and La/Ta = 16.8; Sun and McDonough 1989). In conclusion, the potential sources of mafic magmas in rift zones are thinned SCLM, the convecting mantle beneath the continental plate, or mixtures of the two (Thompson and Gibson 1994). Variability in source region composition is controlled mainly by the level of enrichment; consequently, melt compositions are governed by the interaction between homogeneous asthenospheric mantle, lithosphere, and lower crust. Therefore, fault activity within the tectonic belt may play a more important role than initially expected in terms of controlling the melt composition.

On the basis of this study, magma production may be a function of three constraints: addition of $H_2O \pm CO_2$-rich fluid (produced via metasomatism and carried through fracture systems), decompression melting (deep faults can effectively reduce geological stress in an extensional environment), and increase in mantle temperature (asthenospheric upwelling). During delamination, and with the addition of lower crust, partial melting can release a certain amount of fluid, thereby promoting melting. In addition, large-scale extension over a short period can cause mantle decompression, modifying the geothermal gradient and resulting in partial melting of the lithosphere.

Our data and the related discussion, in combination with the results of previous studies, have culminated in the following genetic model of GHTB that involves three stages (pre-Jurassic, Jurassic, and Cretaceous; Figure 12). During the pre-Jurassic, there existed a thick lower crust that was the result of the Indosinian Collision between the Yangtze and the Cathaysia blocks. Subsequently (in the Early Jurassic), as a result of its higher density (relative to peridotite), this eclogitized lower thickened crust foundered into the lithospheric mantle, inducing upwelling of hot asthenosphere. At this time, adakitic rocks and Cu–(Au) mineralization occurred at Dexing, and the

GHTB mafic dikes were emplaced (Wang *et al*. 2006). Lithospheric extension then continued gradually, resulting in thinning of the GHTB lithosphere and further asthenospheric upwelling. Lower crustal materials then foundered into the lithospheric mantle, before participating in the formation of magma via melting of silica-saturated eclogites. Subsequent decompressional melting of these hybridized lithospheric mantle products resulted in the eruption of 'near-pristine' basaltic melts to form large volcanoes. Uranium mineralization and the emplacement of mafic intrusions and dikes also resulted from this basaltic magma. In addition, partial melting of residual eclogitic lower crust produced the adakitic volcanic rocks found at Pujiang (135–126 Ma; Qin *et al*. 2006).

Conclusions

Based on primary geochronologic, geochemical, and Sr–Nd–Pb isotopic studies of the sampled GHTB mafic dikes, we draw the following conclusions:

(1) Primary radiometric dating demonstrates that the mafic dikes were intruded during the Cretaceous (131–69 Ma). They are all enriched in LREEs and LILEs (Rb, Ba, and Pb), depleted in HFSEs (Nb, Ta, and Ti), and show a wide range of Eu/Eu* values.
(2) The mafic dikes display a wide range of $^{87}Sr/^{86}Sr_i$ (0.704098–0.711026), $^{143}Nd/^{144}Nd_i$ (0.511951–0.512758), εNd_t (–10.4 to +5.6), and Pb isotopic ratios, suggesting their origin from a mantle source that varied from a depleted to an enriched composition, and that was hybridized by foundered lower crust. Subsequent fractionation of olivine, clinopyroxene, plagioclase, and ilmenite or rutile resulted in the generation and emplacement of mafic dikes with negligible crustal contamination.
(3) Lithospheric thinning and asthenospheric upwelling occurred beneath the GHTB during the Cretaceous (131–69 Ma) and was related to foundering of the lower crust.
(4) Fault reactivation and structural constraints within the GHTB played an important role in magmatic evolution and should be the focus of further study.

Acknowledgements

We thank Professor Yuejun Wang and Qiang Wang for their constructive reviews of this manuscript. This research was supported by grants from the National Nature Science Foundation of China (40903018, 40634020, 40773020, and 40673029), the Chinese 973 programme (2007CB411408), and the Science and Technology Foundation of Guizhou Province (No. [2009] 2248). We are grateful to Zhuyin Chu, Chaofeng Li, and Xiuli Wang for their help in analysing Sr, Nd, and Pb isotopes, and to Damin Li for K–Ar dating. We also thank Liang Qi, Jing Hu, and Yan Huang for their work in determining the whole-rock trace element contents.

References

Anderson, D.L., 2006, Speculations on the nature and cause of mantle heterogeneity: Tectonophysics, v. 416, no. 1–4, p. 7–22.
Arndt, N.T., and Goldstein, S.L., 1989, An open boundary between lower continental crust and mantle: Its role in crust formation and crustal recycling: Tectonophysics, v. 161, no. 3–4, p. 201–212.
Carter, A., Roques, D., Bristow, C., and Kinny, P., 2001, Understanding Mesozoic accretion in Southeast Asia: Significance of Triassic thermotectonism (Indosinian orogeny) in Vietnam: Geology, v. 29, no. 3, p. 211–214.
Charvet, J., Lapierre, H., and Yu, Y., 1994, Geodynamic significance of the Mesozoic volcanism of southeastern China: Journal of Southeast Asian Earth Sciences, v. 9, no. 4, p. 387–396.
Chen, A., 1999, Mirror-image thrusting in the South China Orogenic Belt: Tectonic evidence from western Fujian, southeastern China: Tectonophysics, v. 305, no. 4, p. 497–519.
Chen, F.R., and Wang, D.Z., 1995, Comparative anatomy of two contrasting Mesozoic volcanic-intrusive complexes in NE Jiangxi and its vicinities, China: Geochimica, v. 24, no. 2, p. 169-179 (in Chinese).
Chen, J.F., Guo, X.S., Tang, J.F., and Zhou, T.X., 1999, Nd isotopic model ages: Implications of the growth of the continental crust of southeastern China: Journal of Nanjing University (Natural Science), v. 35, no. 06, p. 649–658 (in Chinese).
Chen, J.F., and Jahn, B.M., 1998, Crustal evolution of southeastern China: Nd and Sr isotopic evidence: Tectonophysics, v. 284, no. 1–2, p. 101–133.
Chen, W.F., Chen, P.R., Xu, X.S., and Zhang, M., 2005, Geochemistry of Cretaceous basaltic rocks in South China and the restriction on subduction of the Pacific plate: Science in China: D, v. 35, no. 11, p. 1007–1018 (in Chinese).
Chung, S.L., Jahn, B.M., Chen, S.J., Lee, T., and Chen, C.H., 1995, Miocene basalts in northwestern Taiwan: Evidence for EM-type mantle sources in the continental lithosphere: Geochimica et Cosmochimica Acta, v. 59, no. 3, p. 549–555.
Chung, S.L., Sun, S.S., Tu, K., Chen, C.H., and Lee, C.Y., 1994, Late Cenozoic basaltic volcanism around the Taiwan Strait, SE China: Product of lithosphere-asthenosphere interaction during continental extension: Chemical Geology, v. 112, no. 1–2, p. 1–20.
Cocherie, A., 1986, Systematic use of trace element distribution patterns in log-log diagrams for plutonic suites: Geochimica et Cosmochimica Acta, v. 50, no. 11, p. 2517–2522.
Condie K.C., 1993, Chemical composition and evolution of the upper continental crust: Contrasting results from surface samples and shales: Chemical Geology, v. 104, p. 1–37.
Deng, J.R., and Zhang, Z.P., 1989, Gan-Hang tectonic belt and its geologic significance: Uranium Geology, v. 5, no. 1, p. 15–21 (in Chinese).
Deng, J.R., and Zheng, Z.P., 1997, Discussion on the Precambrian structural framework of the Gan-hang tectonic belt: Uranium Geology, v. 13, no. 6, p. 321–326 (in Chinese).
Deng, J.R., and Zheng, Z.P., 1999, Discussion on regional geotectonic setting of Gan-hang tectonic belt: Uranium Geology, v. 15, no. 2, p. 71–76 (in Chinese).
Deng, P., Shu, L.S., and Xiao, D.H., 2002, A Study on the tectonic basement of Late Mesozoic igneous rocks in southeastern China: Geological Journal of China Universities, v. 8, no. 2, p. 169–179 (in Chinese).

Elkins-Tanton, L., 2005, Continental magmatism caused by lithospheric delamination, in Foulger, G.R., Natland, J.H., Presnall, D.C., and Anderson, D.L., eds., Plates, plumes and paradigms: Geological Society of America Special Paper, p. 449–461.

Escrig, S., Capmas, F., Dupre, B., and Allegre, C.J., 2004, Osmium isotopic constraints on the nature of the DUPAL anomaly from Indian mid-ocean-ridge basalts: Nature, v. 431, no. 7004, p. 59–63.

Fan, W.M., Wang, Y.J., Guo, F., and Peng, T.P., 2003, Mesozoic mafic magmatism in Hunan-Jiangxi Province and the lithospheric extension: Earth Science Frontiers, v. 10, no. 3, p. 159–169 (in Chinese).

Gao, S., Rudnick, R.L., Xu, W.L., Yuan, H.L., Liu, Y.S., Walker, R.J., Puchtel, I.S., Liu, X., Huang, H., Wang, X.R., and Yang, J., 2008, Recycling deep cratonic lithosphere and generation of intraplate magmatism in the North China Craton: Earth and Planetary Science Letters, v. 270, no. 1–2, p. 41–53.

Gao, S., Rudnick, R.L., Yuan, H.L., Liu, X.M., Liu, Y.S., Xu, W.L., Ling, W.L., Ayers, J., Wang, X.C., and Wang, Q.H., 2004, Recycling lower continental crust in the North China craton: Nature, v. 432, no. 7019, p. 892–897.

Ge, X.Y., Li, X.H., and Zhou, H.W., 2003, Geochronology, geochemistry and Sr-Nd isotopes of the Late Cretaceous mafic dike swarms in southern Hainan Island: Geochemica, v. 32, no. 1, p. 11–20 (in Chinese).

Gilder, S.A., Gill, J., Coe, R.S., Zhao, X.X., Liu, Z.W., Wang, G.X., Yuan, K.R., Liu, W.L., Kuang, G.D., and Wu, H.R., 1996, Isotopic and paleomagnetic constraints on the Mesozoic tectonic evolution of south China: Journal of Geophysical Research, v. 101, no. B7, p. 16137–16354.

Gilder, S.A., Keller, G.R., Luo, M., and Goodell, P.C., 1991, Eastern Asia and the Western Pacific Timing and spatial distribution of rifting in China: Tectonophysics, v. 197, no. 2–4, p. 225–243.

Goodell, P.C., Gilder, S., and Fang, X., 1991, A preliminary description of the Gan-Hang failed rift, southeastern China: Tectonophysics, v. 197, no. 2–4, p. 245–255.

Hart, S.R., 1984, A large-scale isotope anomaly in the Southern Hemisphere mantle: Nature, v. 309, no. 5971, p. 753–757.

Hawkesworth, C.J., Blake, S., Evans, P., Hughes, R., MacDonald, R., Thomas, L.E., Turnaer, S.P., and Zellmer, G., 2000, Time scales of crystal fractionation in magma chambers – integrating physical, isotopic and geochemical perspectives: Journal of Petrology, v. 41, no. 7, p. 991–1006.

Hu, G.R., and Zhang, B.T., 1998, Neodymium isotope composition and source materials of the meta-basement in central Jiangxi Province: ACTA Petrologica ET Mineralogica, v. 17, no. 1, p. 35–40 (in Chinese).

Hu, R.Z., Bi, X.W., Peng, J.T., Liu, S., Zhong, H., Zhao, J.H., and Jiang, G.H., 2007, Some problems concerning relationship between Mesozoic-Cenozoic lithospheric extension and uranium metallogenesis in South China: Mineral Deposits, v. 26, no. 2, p. 139–152 (in Chinese).

Hu, R.Z., Bi, X.W., Su, W.C., Peng, J.T., and Li, C.Y., 2004, The relationship between uranium metallogenesis and crustal extension during the Cretaceous-Tertiary in South China: Earth Science Frontier, v. 11, no. 1, p. 153–160 (in Chinese).

Hu, R.Z., Bi, X.W., Zhou, M.F., Peng, J.T., Su, W.C., Liu, S., and Qi, H.W., 2008, Uranium metallogenesis in South China and its relationship to crustal extension during the Cretaceous to Tertiary: Economic Geology, v. 103, no. 3, p. 583–598.

Hua, R.M., Chen, F.R., Zhang, W.L., and Lu, J.J., 2005, Three major metallogenic events in Mesozoic in South China: Mineral Deposits, v. 24, no. 2, p. 99–107 (in Chinese).

Irvine, T.N., and Baragar, W.R.A., 1971, A guide to the chemical classification of the common volcanic rocks: Canadian Journal of Earth Science, v. 8, no. 5, p. 523–548.

Ishizuka, O., Taylor, R.N., Milton, J.A., and Nesbitt, R.W., 2003, Fluid-mantle interaction in an intra-oceanic arc: Constraints from high-precision Pb isotopes: Earth and Planetary Science Letters, v. 211, no. 3–4, p. 221–236.

Jahn, B.M., Wu, F.Y., Lo, C.H., and Tsai, C.H., 1999, Crust-mantle interaction induced by deep subduction of the continental crust: Geochemical and Sr-Nd isotopic evidence from post-collisional mafic-ultramafic intrusions of the northern Dabie complex, central China: Chemical Geology, v. 157, no. 1–2, p. 119–146.

Jenner G.A., Jackson S.E., Fryer B.J., Longerich H.P., Foley S.F. and Green T.H., 1993, Determination of partition coefficients for trace elements in high pressure-temperature experimental run products by laser ablation microprobe-inductively coupled plasma-mass spectrometry (LAM-ICP-MS): Geochimica et Cosmochimica Acta, v. 57, p. 5099–5103.

Jiang, Y.H., Zhao, P., Zhou, Q., Liao, S.Y., and Jin, G.D., 2011, Petrogenesis and tectonic implications of Early Cretaceous S- and A-type granites in the northwest of the Gan-Hang rift, SE China: Lithos, v. 121, no. 1–4, p. 55–73.

Jull, M., and Kelemen, P.B., 2001, On the conditions for lower crustal convective instability: Journal of Geophysics Research, v. 106, no. B4, p. 6423–6446.

Kay, R., and Mahlburg-Kay, S., 1991, Creation and destruction of lower continental crust: Geologische Rundschau, v. 80, no. 2, p. 259–278.

Kimura, G., Takahashi, M., and Kono, M., 1990, Mesozoic collision-extrusion tectonics in eastern Asia: Tectonophysics, v. 181, no. 1–4, p. 15–23.

Le Bas, M.J., Le Maitre, R.W., Streckeisen, A., and Zanettin, B., 1986, A chemical classification of volcanic rocks based on the total alkali-silica diagram: Journal of Petrology, v. 27, no. 3, p. 745–750.

le Roex A.P., 1986, Geochemical correlation between southern African kimberlites and South Atlantic hotspots: Nature, v. 324, p. 243–245.

Li, W.X., and Zhou, X.M., 2001, Subduction of the palaeo-Pacific plate and origin of late Mesozoic igneous rocks in southeastern China – Some supplement evidence for the model of lithosphere subduction and underplating of mafic magma: Geotectonica et Metallogenia, v. 25, no. 1, p. 55–63 (in Chinese).

Li, X.H., 1990, Genesis of intermediate-basic-dykes in Zhuguang body: Evidences from Sr, Nd and O isotopes: Chinese Science Bulletin, v. 35, no. 16, p. 1247–1249 (in Chinese).

Li, X.H., Chen, Z.G., Liu, D.Y., and Li, W.X., 2003, Jurassic gabbro-granite-syenite suites from Southern Jiangxi Province, SE China: Age, origin, and tectonic significance: International Geology Review, v. 45, no. 10, p. 898–921.

Li, X.H., Chung, S.L., Zhou, H.W., Lo, C.H., Liu, Y., and Chen, C.H., 2004, Jurassic intraplate magmatism in southern Hunan-eastern Guangxi: $^{40}Ar/^{39}Ar$ dating, geochemistry, Sr-Nd isotopes and implications for the tectonic evolution of SE China: Geological Society, London, Special Publications, v. 226, no. 1, p. 193–215.

Li, X.H., Hu, R.Z., and Bin., R., 1997, Geochronology and geochemistry of Cretaceous mafic dikes from northern Guangdong, SE China: Geochemica, v. 26, no. 2, p. 14–31 (in Chinese).

Li, X.H., Li, W.X., and Li, Z.X., 2007, On the genetic classification and tectonic implications of the early Yanshanian

granitoids in the Nanling Range, South China: Chinese Science Bulletin, v. 52, no. 14, p. 1873–1885.
Li, Z.X., and Li, X.H., 2007, Formation of the 1300-km-wide intracontinental orogen and postorogenic magmatic province in Mesozoic South China: A flat-slab subduction model: Geology, v. 35, no. 2, p. 179–182.
Li, Z.X., Li, X.H., Zhou, H., and Kinny, P.D., 2002, Grenvillian continental collision in south China: New SHRIMP U-Pb zircon results and implications for the configuration of Rodinia: Geology, v. 30, no. 2, p. 163–166.
Liu, S., 2004, The Mesozoic magmatism and crustal extension in Shandong Province, China-additionally discussing the relationship between lamprophyres and gold mineralization: Guiyang, Institute of Geochemistry, Chinese Academy of Science, p. 1–96 (in Chinese).
Liu, S., Hu, R., Gao, S., Feng, C., Feng, G., Coulson, I.M., Li, C., Wang, T., and Qi, Y., 2010, Zircon U-Pb age and Sr-Nd-Hf isotope geochemistry of Permian granodiorite and associated gabbro in the Songliao Block, NE China and implications for growth of juvenile crust: Lithos, v. 114, no. 3–4, p. 423–436.
Liu, S., Hu, R., Gao, S., Feng, C., Yu, B., Feng, G., Qi, Y., Wang, T., and Coulson, I.M., 2009a, Petrogenesis of Late Mesozoic mafic dykes in the Jiaodong Peninsula, eastern North China Craton and implications for the foundering of lower crust: Lithos, v. 113, no. 3–4, p. 621–639.
Liu, S., Hu, R., Gao, S., Feng, C., Yu, B., Qi, Y., Wang, T., Feng, G., and Coulson, I.M., 2009b, Zircon U-Pb age, geochemistry and Sr-Nd-Pb isotopic compositions of adakitic volcanic rocks from Jiaodong, Shandong Province, Eastern China: Constraints on petrogenesis and implications: Journal of Asian Earth Sciences, v. 35, no. 5, p. 445–458.
Liu, S., Hu, R., Gao, S., Feng, C., Zhong, H., Qi, Y., Wang, T., Feng, G., and Yang, Y., 2011, U-Pb zircon ages, geochemical and Sr-Nd-Pb isotopic constraints on the dating and origin of intrusive complexes in the Sulu orogen, eastern China: International Geology Review, p. v. 53, no. 1, p. 61–83.
Liu, S., Hu, R.Z., Gao, S., Feng, C.X., Qi, L., Zhong, H., Xiao, T.F., Qi, Y.Q., Wang, T., and Coulson, I.M., 2008a, Zircon U-Pb geochronology and major, trace elemental and Sr-Nd-Pb isotopic geochemistry of mafic dykes in western Shandong Province, east China: Constrains on their petrogenesis and geodynamic significance: Chemical Geology, v. 255, no. 3–4, p. 329–345.
Liu, S., Hu, R.Z., Gao, S., Feng, C.X., Qi, Y.Q., Wang, T., Feng, G.Y., and Coulson, I.M., 2008b, U-Pb zircon age, geochemical and Sr-Nd-Pb-Hf isotopic constraints on age and origin of alkaline intrusions and associated mafic dikes from Sulu orogenic belt, Eastern China: Lithos, v. 106, no. 3–4, p. 365–379.
Liu, S., Zou, H.B., Hu, R.Z., Zhao, J.H., and Feng, C.X., 2006, Mesozoic mafic dikes from the Shandong Peninsula, North China Craton: Petrogenesis and tectonic implications: Geochemical Journal, v. 40, no. 2, p. 181–195.
Lustrino, M., 2005, How the delamination and detachment of lower crust can influence basaltic magmatism: Earth-Science Reviews, v. 72, no. 1–2, p. 21–38.
Ma, C.X., and Xiang, X.K., 1993, Preliminary study of the Nd isotopic model ages of the Precambrian metamorphic stratum in Northeastern Jiangxi Province: Scientia Geologica Sinica, v. 28, no. 2, p. 145–150 (in Chinese).
Mao, J.R., Chen, R., Li, J.Y., Ye, H.M., and Zhao, X.L., 2006, Geochronology and geochemical characteristics of late Mesozoic granitic rocks from southwestern Fujian and their tectonic evolution: Acta Petrologica Sinica, v. 22, no. 6, p. 1723–1734 (in Chinese).
Mao, J.W., Xie, G.Q., Li, X.F., Zhang, C.Q., and Mei, Y.X., 2004, Mesozoic large scale mineralization and multiple lithospheric extension in South China: Earth Science Frontiers, v. 11, no. 1, p. 45–55.
Maruyama, S., and Send, T., 1986, Orogeny and relative plate motions: Example of the Japanese Islands: Tectonophysics, v. 127, no. 3–4, p. 305–329.
Menzies, M., Xu, Y.G., Zhang, H.F., and Fan, W.M., 2007, Integration of geology, geophysics and geochemistry: A key to understanding the North China Craton: Lithos, v. 96, no. 1–2, p. 1–21.
Mohr, P.A., 1987, Crustal contamination in mafic sheets: A summary, in Halls, H.C., and Fahrig, W.C., eds., Mafic dyke swarms: Special Publication-Geological Association of Canada, p. 75–80.
Pearce, J.A., and Norry, M.J., 1979, Petrogenetic implications of Ti, Zr, Y, and Nb variations in volcanic rocks: Contributions to Mineralogy and Petrology, v. 69, p. 33–47.
Plank, T., and Langmuir, C.H., 1998, The chemical composition of subducting sediment and its consequences for the crust and mantle: Chemical Geology, v. 145, no. 3–4, p. 325–394.
Qi, L., Hu, J., and Gregoire, D.C., 2000, Determination of trace elements in granites by inductively coupled plasma mass spectrometry: Talanta, v. 51, no. 3, p. 507–513.
Qin, S.C., Fan, W.M., Guo, F., Li, C.W., and Gao, X.F., 2006, Petrogenesis of late Mesozoic adakitic andesites from Pujiang area in Zhejiang Province, eastern China: Acta Petrologica Sinica, v. 22, no. 9, p. 2305–2314 (in Chinese).
Ratschbacher, L., Hacker, B.R., Webb, L.E., McWilliams, M., Ireland, T., Dong, S.W., Calvert, A., Chateigner, D., and Wenk, H.R., 2000, Exhumation of the ultrahigh-pressure continental crust in east central China: Cretaceous and Cenozoic unroofing and the Tan-Lu fault: Journal of geophysical research, v. 105, no. B6, p. 13303–13338.
Rudnick, R.L., and Fountain, D.M., 1995, Nature and composition of the continental crust: A lower crustal perspective: Reviews of Geophysics, v. 33, no. 3, p. 267–309.
Rudnick, R.L., and Gao, S., 2003, Composition of the continental crust: Treatise on geochemistry, v. 3, p. 1–64.
Shao, F., 2004, Edge Uranium Metallogenic in Gan-Hang tectonic belt: Uranium Geology of East China, v. 1, p. 7–11 (in Chinese).
Shu, L.S., 2006, Predevonian tectonic evolution of South China: From Cathaysian block to Caledonian Period Folded Orogenic Belt: Journal of China Universities, v. 12, no. 4, p. 418–431 (in Chinese).
Staudigel, H., Plank, T., White, B., and Schmincke, H.U., 1996, Geochemical fluxes during seafloor alteration of the basaltic upper oceanic crust: DSDP sites 417 and 418: Geophysical monograph, v. 96, p. 19–38.
Steiger, R.H., and Jäer, E., 1977, Subcommission on geochronology: Convention on the use of decay constants in geo- and cosmochronology: Earth and Planetary Science Letters, v. 36, no. 3, p. 359–362.
Sun S.S. and McDonough W.F., 1989, Chemical and isotopic systematics of oceanic basalts: implications for mantle composition and processes: Geological Society, London, Special Publications, v. 42, p. 313–345.
Taylor, S.R., and McLennan, S.M., 1985, The continental crust: Its composition and evolution: Hoboken, NJ, Blackwell Scientific Publications, p. 1–328 pp.
Thompson, R.N., and Gibson, S.A., 1994, Magmatic expression of lithospheric thinning across continental rifts: Tectonophysics, v. 233, no. 1–2, p. 41–68.

Tu, K., Flower, M.F.J., Carlson, R.W., Zhang, M., and Xie, G., 1991, Sr, Nd, and Pb isotopic compositions of Hainan basalts (South China); implications for a subcontinental lithosphere Dupal source: Geology, v. 19, no. 6, p. 567–569.

Wang D.Z. and Shen W.Z., 2003, Genesis of granitoids and crustal evolution in southeast China: Earth Science Frontiers, v. 10, p. 209–220 (in Chinese).

Wang, D.Z., 2004, The study of granitic rocks in South China: Looking back and forward: Geological Journal of China Universities, v. 10, no. 3, p. 305–314 (in Chinese).

Wang, Q., Wyman, D.A., Xu, J.F., Zhao, Z.H., Jian, P., and Zi, F., 2007, Partial melting of thickened or delaminated lower crust in the middle of Eastern China: Implications for Cu-Au mineralization: The Journal of Geology, v. 115, no. 2, p. 149–163.

Wang, Q., Xu, J.F., Jian, P., Bao, Z.W., Zhao, Z.H., Li, C.F., Xiong, X.L., and Ma, J.L., 2006, Petrogenesis of adakitic porphyries in an extensional tectonic setting, Dexing, South China: Implications for the genesis of porphyry copper mineralization: Journal of Petrology, v. 47, no. 1, p. 119–144.

Wang, Q., Zhao, Z.H., Jian, P., Xiong, X.L., Bao, Z.W., Dai, T.M., Xu, J.F., and Ma, J.L., 2005a, Geochronology of Cretaceous A-type granitoids or alkaline intrusive rocks in the hinterland, South China: Constraints for late-Mesozoic tectonic evolution: Acta Petrologica Sinica, v. 21, no. 3, p. 795–808 (in Chinese).

Wang, Q., Zhao, Z.H., Jian, P., Xu, J.F., Bao, Z.W., and Ma, J.L., 2004, SHRIMP zircon geochronology and Nd-Sr isotopic geochemistry of the Dexing granodiorite porphyries: Acta Petrologica Sinica, v. 20, no. 2, p. 315–324 (in Chinese).

Wang, Y.J., Fan, W.M., Cawood, P.A., and Li, S.Zh., 2008, Sr-Nd-Pb isotopic constraints on multiple mantle domains for Mesozoic mafic rocks beneath the South China Block hinterland: Lithos, v. 106, no. 3–4, p. 297–308.

Wang, Y.J., Fan, W.M., Guo, F., Peng, T.P., and Li, C.W., 2003, Geochemistry of Mesozoic mafic rocks adjacent to the Chenzhou-Linwu fault, South China: Implications for the lithospheric boundary between the Yangtze and Cathaysia Blocks: International Geology Review, v. 45, no. 3, p. 263–286.

Wang, Y.J., Fan, W.M., Peng, T.P., and Guo, F., 2005b, Elemental and Sr–Nd isotopic systematics of the early Mesozoic volcanic sequence in southern Jiangxi Province, South China: Petrogenesis and tectonic implications: International Journal of Earth Sciences, v. 94, no. 1, p. 53–65.

White, W.M., Hofmann, A.W., and Puchelt, H., 1987, Isotope geochemistry of Pacific mid-ocean ridge basalt: Journal of Geophysical Research, v. 92, no. B6, p. 4881–4894.

Winchester, J.A., and Floyd, P.A., 1977, Geochemical discrimination of different magma series and their differentiation products using immobile elements: Chemical Geology, v. 20, p. 325–343.

Wu, F.Y., Ce, W.C., Sun, D.Y., and Guo, C.L., 2003, Discussion on the lithospheric thinning in eastern China: Earth Science Frontiers, v. 10, no. 3, p. 51–60 (in Chinese).

Xie, D.K., 1996, Continental crust growth and mantle plume structure, South China: Beijing, The Geological Publishing House, p. 1–257 (in Chinese).

Xie, G.Q., 2003, Late Mesozoic and Cenozoic Mafic Dikes (bodies) from Southeastern China: Geological and geochemical characteristics and its geodynamics – a case of Jiangxi Province: Guiyang, Institute of Geochemistry, Chinese Academy of Science, p. 1–126 (in Chinese).

Xie, G.Q., Hu, R.Z., Mao, J.W., Pirajno, F., Li, R.L., Cao, J.J., Jiang, G.H., and Zhao, J.H., 2006, K-Ar dating, geochemical, and Sr-Nd-Pb isotopic systematics of Late Mesozoic mafic dikes, southern Jiangxi Province, Southeast China: Petrogenesis and tectonic implications: International Geology Review, v. 48, no. 11, p. 1023–1051.

Xu, X.S., 2008, Several problems worthy to be noticed in the research of granites and volcanic rocks in SE China: Geological Journal of China Universities, v. 14, no. 3, p. 283–294 (in Chinese).

Xu, Y.G., Ross, J.V., and Mercier, J.C.C., 1993, The upper mantle beneath the continental rift of Tanlu, Eastern China: Evidence for the intra-lithospheric shear zones: Tectonophysics, v. 225, no. 4, p. 337–360.

Yan J., Chen J.F., Yu G., Qian H. and Zhou T.X., 2003, Pb isotopic characteristics of Late Mesozoic mafic rocks from the lower Yangtze region: evidence for enriched mantle: Geological Journal of China Universities, v. 9, p. 195–206 (in Chinese).

Yan, J., and Chen, J.F., 2007, Geochemistry of Qingshan formation volcanic rocks from Jiaolai basin, eastern Shandong Province: Petrogenesis and geological significance: Geochimica, v. 36, no. 1, p. 1–10 (in Chinese).

Yu, X.Q., Shu, L.S., Yan, T.Z., Yu, Y.W., Zu, F.P., and Wang, B., 2004, Geochemistry of basalts of late period of Early Cretaceous from Jiangshan-Guangfeng, SE China and its tectonic significance: Geochimica, v. 33, no. 5, p. 465–476 (in Chinese).

Yu, X.Q., Wu, G.G., Shu, L.S., Yan, T.Z., Zhang, D., and Di, Y.J., 2006, The Cretaceous tectonism of the Gan-Han Tectonic Belt, southeastern China: Earth Science Frontier, v. 13, no. 3, p. 3143 (in Chinese).

Zhang, X.F., 1999a, Formation and evolution of Mesozoic volcanic basin in Gan-hang tectonic belt: Uranium Geology, v. 15, no. 1, p. 18–23 (in Chinese).

Zhang, X.F., 1999b, Formation and evolution of Mesozoic red basins in Ganhang tectonic belt: Uranium Geology, v. 15, no. 2, p. 77–85 (in Chinese).

Zhang, X.F., 2004, The cause of Gan-Hang tectonic belt and typical faults in red basin of eastern China: Journal of East China uranium, v. 1, p. 1–6 (in Chinese).

Zhao, J.H., 2004, Chronology and geochemistry of mafic rocks from Fujian Province: Implications for the mantle evolution of SE China since Late Mesozoic: Guiyang, Institute of Geochemistry, Chinese Academy of Science, p. 1–107 (in Chinese).

Zhao, J.H., Hu, R.Z., and Liu, S., 2004, Geochemistry, petrogenesis, and tectonic significance of Mesozoic mafic dikes, Fujian Province, Southeastern China: International Geology Review, v. 46, no. 6, p. 542–557.

Zhao, J.H., Hu, R.Z., Zhou, M.F., and Liu, S., 2007, Elemental and Sr-Nd-Pb isotopic geochemistry of Mesozoic mafic intrusions in southern Fujian Province, SE China: Implications for lithospheric mantle evolution: Geological Magazine, v. 144, no. 6, p. 937–952.

Zhou, J.C., and Chen, R., 2000, Study of late Mesozoic interaction between crust and mantle in coastland of Zhejiang and Fujian Province: Progress in Natural Science, v. 10, no. 6, p. 571–574 (in Chinese).

Zhou, J.C., and Chen, R., 2001, Geochemistry of late Mesozoic interaction between crust and mantle in southeastern Fujian Province: Geochimica, v. 30, no. 6, p. 547–558 (in Chinese).

Zhou, X.M., 2003, My thinking about granite geneses of South China: Geological Journal of China Universities, v. 9, no. 4, p. 556–565 (in Chinese).

Zhou, X.M., and Li, W.X., 2000, Origin of Late Mesozoic igneous rocks in Southeastern China: Implications for lithosphere subduction and underplating of mafic magmas: Tectonophysics, v. 326, no. 3–4, p. 269–287.

Zhou, X.M., Sun, T., Shen, W.Z., Shu, L.S., and Niu, Y.L., 2006, Petrogenesis of Mesozoic granitoids and volcanic rocks in South China: A response to tectonic evolution: Episodes, v. 29, no. 1, p. 26–33.

Zhou, X.M., and Zhu, Y.H., 1993, Late Proterozoic collisional orogen and geosuture in Southeastern China: Petrological evidence: Chinese Journal of Geochemistry, v. 12, no. 3, p. 239–251 (in Chinese).

Zhu, W.G., Zhong, H., Li, X.H., He, D.F., Song, X.Y., Ren, T., Chen, Z.Q., Sun, H.S., and Liao, J.Q., 2010, The Early Jurassic mafic-ultramafic intrusion and A-type granite from northeastern Guangdong, SE China: Age, origin, and tectonic significance: Lithos, v. 119, no. 3–4, p. 313–329.

Zindler, A., and Hart, S., 1986, Chemical Geodynamics: Annual Review of Earth and Planetary Sciences, v. 14, no. 1, p. 493–571.

Zou, H.B., Zindler, A., Xu, X.S., and Qi, Q., 2000, Major, trace element, and Nd, Sr and Pb isotope studies of Cenozoic basalts in SE China: Mantle sources, regional variations, and tectonic significance: Chemical Geology, v. 171, no. 1–2, p. 33–47.